The rheology of non-dilute dispersions of highly deformable viscoelastic particles in Newtonian fluids

Reza Avazmohammadi and Pedro Ponte Castañeda †

Department of Mechanical Engineering and Applied Mechanics, University of Pennsylvania, Philadelphia, PA 19104-6315, USA

(Received 6 January 2015)

We present a model for the rheological behavior of non-dilute suspensions of initially spherical, viscoelastic particles in viscous fluids under uniform, Stokes flow conditions. The particles are assumed to be neutrally buoyant, Kelvin-Voigt solids undergoing time-dependent, finite deformations, and exhibiting generalized neo-Hookean behavior in their purely elastic limit. We investigate the effects of the shape dynamics and constitutive properties of the viscoelastic particles on the macroscopic rheological behavior of the suspensions. The proposed model makes use of known homogenization estimates for composite material systems consisting of random distributions of aligned ellipsoidal particles with prescribed two-point correlation functions to generate corresponding estimates for the instantaneous (incremental) response of the suspensions, together with appropriate evolution laws for the relevant microstructural variables. To illustrate the essential features of the model, we consider two special cases: (1) extensional flow, and (2) simple shear flow. For each case, we provide the time-dependent response, and when available, the steady-state solution for the average particle shape and orientation, as well as for the effective viscosity and normal stress differences in the suspensions. The results exhibit shear thickening for extensional flows and shear thinning for simple shear flows, and it is found that the volume fraction and constitutive properties of the particles significantly influence the rheology of the suspensions under both types of flows. In particular, for extensional flows, suspensions of particles with finite extensibility constraints are always found to reach a steady state, while this is only the case at sufficiently low strain rates for suspensions of (less realistic) neo-Hookean particles, as originally reported by Roscoe (J. Fluid Mech., vol. 28, 1967, pp. 273–293) and Gao et al. (J. Fluid Mech., vol. 687, 2011, pp. 209-237). For shear flows, viscoelastic particles with high viscosities can experience a damped oscillatory motion of decreasing amplitude before reaching the steady state.

1. Introduction

Suspensions of interacting *deformable* particles in a fluid are used in numerous applications of current interest (e.g., tissue engineering, drug delivery, paints and coatings), and they constitute a large class of naturally existing mixtures as well (e.g., blood and milk). Among them, solid-fluid mixtures consisting of large numbers of deformable, micro-scaled, solid particles suspended in Newtonian fluids are of particular importance. Well-known examples of these mixtures include suspensions of red blood cells in blood plasma (Skalak *et al.* 1989), and suspensions of microgel particles in a solvent (Pal 2010). When subjected to shear flows, the suspended particles undergo significant changes in shape and orientation, and this evolution of the microstructure is expected to have a strong

† Email address for correspondence: ponte@seas.upenn.edu

influence on the macroscopic rheological properties of the suspension. It follows that sound models for the constitutive behavior of such suspensions must properly account for appropriate microstructural variables, such as the average shape and orientation of the particles, as well as for the constitutive nonlinearities associated with the mechanical response of the particles.

In the past decades, a vast amount of research has focused on estimating the effective viscosity of dilute and non-dilute suspensions of *rigid* particles (Einstein 1906; Jeffery 1922; Saito 1950; Krieger & Dougherty 1959; Keller *et al.* 1967; Frankel & Acrivos 1967; Batchelor 1970; Batchelor & Green 1972; Jeffrey & Acrivos 1976; Gadala-Maria & Acrivos 1980; Brady & Bossis 1985; Phung *et al.* 1996; Stickel & Powell 2005, to cite only a few). By comparison, fewer studies deal with the rheology of suspensions of dilute and non-dilute concentrations of *deformable* solid particles in a Newtonian fluid. Among the pioneering studies, Fröhlich & Sack (1946) considered suspensions of elastic spherical particles in a Newtonian fluid undergoing a pure extensional flow and derived constitutive equations relating the macroscopic extensional stress and the applied strain rate for small deformations of the microstructure. Cerf (1952) investigated a suspension of spheres with special viscoelastic properties in a viscous liquid under oscillatory motion of small amplitude. More than a decade later, Roscoe (1967) studied the rheological behavior of *dilute* suspensions of solid viscoelastic spheres in a Newtonian fluid within the context of finite strains. In that work, which was limited to steady-state (SS) responses, Roscoe obtained the effective viscosity and normal stress differences for the suspension as functions of the solid and liquid material properties and the flow conditions. In addition, Roscoe demonstrated that, for initially spherical particles and shear-flow conditions, steady-state solutions are possible, under certain conditions, such that the particle deforms into an ellipsoid of fixed orientation, and the material within the ellipsoid undergoes a tank-treading motion deforming and rotating continuously with uniform velocity gradient and stress. In closely related work, Goddard & Miller (1967) investigated the time-dependent behavior of a viscoelastic sphere in a Newtonian fluid within the limits of *small deformations* of the particle. Based on the coupled solutions for the flow field around the particle and the deformation of the particle, they derived a constitutive equation for the rheological behavior of suspensions of slightly deformed spheres in the dilute limit. In the regime of non-dilute concentrations of particles but, again, within the *small deformations* limit, Goddard (1977) generalized the analysis of Frankel & Acrivos (1967) for highly concentrated suspensions of rigid particles to account for the effect of small deformation of the particles on the rheology of the suspension. In addition, Snabre & Mills (1999) made use of an effective medium approximation for an isotropic dispersion of rigid spheres, together with an estimate for the effect of particle deformations on the maximum packing fraction of the suspension under flow, to develop a model for the effective shear viscosity of concentrated suspensions of viscoelastic particles. This model was able to the describe the effective viscosity of suspensions of red cells, but due to the implicit isotropy assumptions cannot account for the development of normal stress differences in the suspension. Again, within the context of small deformations, Pal (2003) derived a semi-empirical equation for the effective viscosity of non-dilute suspensions of elastic particles by means of the differential effective medium approximation, together with the constitutive model developed by Goddard & Miller (1967) for dilute suspensions of spherical, elastic particles. The author found good agreement with experimental data for the effective shear viscosity of un-aggregated red cells in saline solution, but this model also ignores the development of normal shear stress differences under simple shear loading. There has also been a considerable amount of work on suspensions of viscous droplets or emulsions, where it is crucial to account for interfacial tension between the

two fluids (see, for example, Taylor 1932; Oldroyd 1953; Keller *et al.* 1967; Bilby *et al.* 1975; Palierne 1990; Lowenberg & Hinch 1996; Almusallam *et al.* 2000; Tucker & Moldenaers 2002; Vlahovska *et al.* 2009). In addition, numerous works have been published for suspensions of capsules (e.g., Barthès-Biesel 1980; Barthès-Biesel & Rallison 1981; Keller & Skalak 1982; Ramanujan & Pozrikidis 1998; Lac *et al.* 2004), as well as for vesicles (e.g., Danker & Misbah 2007; Ghigliotti *et al.* 2010; Zhao & Shaqfeh 2013; Abreu *et al.* 2014).

As demonstrated by several of the above-mentioned studies, the constitutive properties of the particles strongly influence the rheology of suspensions of deformable particles in a viscous fluid. Although these studies can capture to some extent the influence of particle deformation on the effective properties of the suspensions, they are confined to small strains and/or dilute concentrations. Indeed, rheological models that can address general morphologies and particle volume fractions, as well as general constitutive behavior and finite deformations for the deformable particles in the suspension are still largely lacking. Recently, Gao *et al.* (2011) investigated the rheology of dilute suspensions of neo-Hookean particles in a Newtonian fluid under Stokes flow conditions. Making use of a polarization technique, the authors developed an *exact* analytical estimate describing the finite-strain, time-dependent response of a *neo-Hookean elastic* particle in a viscous shear flow. (This result has recently been verified numerically for initially spherical particles by Villone *et al.* (2014).) Gao *et al.* (2011) found that the (time-dependent) "excess" viscosity of the *dilute* suspensions of such particles exhibits strong coupling with the large changes in the particle shape and orientation leading to a shear thinning effect. Most recently, they made use of their model to study the rheology of dilute suspensions of neo-Hookean particles in extensional flows (Gao *et al.* 2013), and found a shear-thickening effect instead. In addition, Gao *et al.* (2012) showed that it was possible to have three types of motions—steady-state, "trembling" (oscillatory), and "tumbling"—for dilute concentration of *elastic* particles, depending on the shear rate, elastic shear modulus, and initial particle shape.

With the perspectives afforded by the work of Gao *et al.* (2011) for *dilute* suspensions of *elastic* particles in mind, the goal of the present work is to investigate the time-dependent rheological properties of *non-dilute* suspensions of *deformable viscoelastic* particles in the regime of arbitrarily large deformations. In particular, we investigate the effective rheological response, as well as the microstructure evolution, in suspensions of initially spherical, nonlinear KV viscoelastic particles with generalized neo-Hookean elastic behavior in a Newtonian viscous fluid subjected to macroscopically uniform flows. We assume that the characteristic size of the particles is larger than $1\,\mu m$ so that we can neglect Brownian forces acting on the particles. Also, we confine our attention to the Stokes flow regime (i.e., $Re \to 0$), where viscous forces dominate over inertial effects. We develop a homogenization model to obtain time-dependent estimates, and when available, steady-state estimates for the rheological behavior of these suspensions. The model is based on the Hashin-Shtrikman-Willis (HSW) homogenization theory (Hashin & Shtrikman 1963; Willis 1977), which was originally developed for elastic composite materials. More specifically, we make use of the bounds of Ponte Castañeda & Willis (1995) for composites consisting of aligned ellipsoidal particles that are distributed randomly with (generally different) "ellipsoidal" angular dependence for the two-point correlations of the particle centers in a matrix of a different material. Thus, these bounds incorporate dependence on both the shape and orientation of the particles, as well as on the "shape" and "orientation" of the two-point correlation function for their distribution, through two independent microstructural tensors. However, they cannot distinguish between mono- and poly-disperse distributions of particles, and must hold for all possible particle size

distributions—although they are known to be more appropriate for poly-disperse distributions. As a consequence, these bounds cannot be directly compared with the estimates of Batchelor & Green (1972) and Chen & Acrivos (1978) for *mono-disperse* distributions of rigid spherical particles. The homogenization estimates of Ponte Castañeda & Willis (1995) were generalized for two-phase viscous systems by Kailasam *et al.* (1997) and Kailasam & Ponte Castañeda (1998), and used to generate estimates for the deformation inside the particles, which when combined with nonlinear equations for the evolution of the shape and orientation of the particles, can in turn be used to characterize the macroscopic rheological behavior of such purely viscous suspensions in uniform flows.

The structure of the paper is as follows. Section 2 addresses the constitutive behavior of the deforming solid particles and the types of particulate microstructures considered in this work. In section 3, we lay out the homogenization strategy. We first provide results for the *instantaneous* macroscopic stress in the suspensions in terms of the average elastic stress and strain rate inside the particles, which can in turn be related to the macroscopic strain rate in the suspension. Next, we confine our attention to suspensions of initially spherical particles that are initially distributed with statistical isotropy. Then, using consistent homogenization estimates for the *average* strain-rate and vorticity tensors in the particles, we develop evolution equations for the *average* particle shape and orientation. For simplicity, we assume that the evolution of the shape and orientation of the angular dependence of the two-point correlation functions (for the particle centers) is the same as that for the particles. Section 4 provides explicit expressions for steady-state conditions for non-dilute concentration of Kelvin-Voigt and purely elastic particles, thus generalizing the results of Roscoe (1967) for dilute concentrations. In section 5, we apply our model for two important special cases. First, we consider the problem of suspensions of initially spherical particles in an extensional flow, and provide representative numerical examples, as well as closed-form results for steady-state conditions. Second, we consider the application of the model to suspensions of initially spherical particles in a shear flow. Finally, some conclusions are drawn in section 6.

2. Suspensions of viscoelastic particles in a viscous fluid

As already mentioned, in this work, we consider *random* dispersions of (solid) nonlinear viscoelastic particles in a Newtonian fluid (matrix phase). The solid particles and fluid phases are incompressible and have the same density, so that the particles are neutrally buoyant in the fluid. In this section, we describe in some detail the constitutive behavior of the homogeneous matrix and particle phases in the suspension, as well as for the microstructures of interest. Following this section, our aim will be to deliver estimates for the macroscopic rheological response and associated microstructure evolution in these suspensions under uniform flow conditions.

We begin with a quick review of the basic kinematic relations, in particular, to fix the notation. Under the application of mechanical loadings, a material point $\mathbf{X}$ in the reference configuration moves to a new point $\mathbf{x}$ at time t in the deformed configuration of the particle. In the Lagrangian description of the motion, the deformation is described by the map $\mathbf{x}(\mathbf{X}, t)$, assumed to be continuous and one-to-one. The deformation gradient tensor $\mathbf{F} = \mathrm{Grad}\,\mathbf{x}$ (with Cartesian components $F_{ij} = \partial x_i/\partial X_j$) then serves to characterize the deformation of the material, and is such that $\mathbf{F} = \mathbf{RU} = \mathbf{VR}$, where $\mathbf{R}$ is the rotation, and $\mathbf{U}$ and $\mathbf{V}$ are the right- and left-stretch tensors, respectively. We will also make use of the right and left Cauchy-Green tensors, given by $\mathbf{C} = \mathbf{F}^T\mathbf{F} = \mathbf{U}^2$ and $\mathbf{B} = \mathbf{F}\mathbf{F}^T = \mathbf{V}^2$, respectively. ($\mathbf{B}$ is also known as the Finger tensor.) Correspondingly, in the Eulerian description, the motion is described by the velocity field $\mathbf{v}(\mathbf{x}, t)$, such that the Eulerian

strain rate and vorticity tensors are given by $\mathbf{D} = \frac{1}{2}\left(\mathbf{L} + \mathbf{L}^T\right)$ and $\mathbf{W} = \frac{1}{2}\left(\mathbf{L} - \mathbf{L}^T\right)$, respectively, where $\mathbf{L} = \operatorname{grad}\mathbf{v}$ is the velocity gradient, which is related to the deformation gradient by $\mathbf{L} = \dot{\mathbf{F}}\mathbf{F}^{-1}$, with $\dot{\mathbf{F}}$ denoting the (material) time derivative of $\mathbf{F}$.

2.1. *Constitutive behavior of the phases*

We assume that the suspended particles are homogeneous and made of deformable, incompressible, isotropic solids. We consider particles with viscoelastic behavior and make use of a generalized Kelvin-Voigt (KV) model to describe their constitutive response. This model consists of a hyperelastic spring and a dashpot connected in parallel. (More general models, such as Jeffreys model, could be considered at the expense of somewhat more complicated expressions.) We will also consider suspensions of purely elastic particles, which are one limiting case of the KV particles. For the incompressible KV material, the Cauchy stress $\boldsymbol{\sigma}$ can be written as (Joseph 1990)

$$\boldsymbol{\sigma} = -p_0\mathbf{I} + \boldsymbol{\tau}, \quad \boldsymbol{\tau} = \boldsymbol{\tau}_e + \boldsymbol{\tau}_v, \tag{2.1}$$

where p_0 is an arbitrary hydrostatic pressure associated with the incompressibility constraint, and $\boldsymbol{\tau}_e$ and $\boldsymbol{\tau}_v$ are the elastic and viscous parts of the total "extra" stress tensor $\boldsymbol{\tau}$ in the particle (which need not be deviatoric in general, $\operatorname{tr}(\boldsymbol{\tau}) \neq 0$.) Note that the actual hydrostatic pressure p is given by $p = p_0 - \operatorname{tr}\boldsymbol{\tau}$.

The elastic stress may be described in terms of a stored-energy function ψ, which, on account of frame invariance, is a function of $\mathbf{C}$, via

$$\boldsymbol{\tau}_e = 2\mathbf{F}\frac{\partial\psi(\mathbf{C})}{\partial\mathbf{C}}\mathbf{F}^T, \quad \det(\mathbf{F}) = 1. \tag{2.2}$$

In addition, elastic isotropy (and incompressibility) implies that ψ depends on $\mathbf{C}$ through its first two invariants. For simplicity, in this work, we will consider *generalized neo-Hookean* behavior such that $\psi(\mathbf{C}) = g(I)$, where $I = \operatorname{tr}(\mathbf{C})$ and g is a generally nonlinear function of I satisfying the requirements that $g(3) = 0$, $g'(3) = \mu/2$, where μ is the ground state shear modulus of the elastic particle. Then, the elastic extra stress tensor $\boldsymbol{\tau}_e$ in (2.2) can be expressed as

$$\boldsymbol{\tau}_e = 2\,g'(I)\,\mathbf{B} - \mu\,\mathbf{I}, \tag{2.3}$$

where the term proportional to μ arises from the linearization requirements at the ground state (i.e., $\boldsymbol{\tau}_e(\mathbf{I}) = \mathbf{0}$).

Making use of the fact that (Joseph 1990)

$$\overset{\triangledown}{\mathbf{B}} = \frac{\mathrm{D}\,\mathbf{B}}{\mathrm{D}t} - \mathbf{L}\mathbf{B} - \mathbf{B}\mathbf{L}^T = \mathbf{0}, \tag{2.4}$$

a *rate* (hypo-elastic) form of equation for the elastic constitutive relation (2.3) may be obtained in terms of the upper-convected (or Oldroyd) time derivative such that

$$\overset{\triangledown}{\boldsymbol{\tau}}_e = \dot{\boldsymbol{\tau}}_e - \mathbf{L}\boldsymbol{\tau}_e - \boldsymbol{\tau}_e\mathbf{L}^T = 4\,g''\operatorname{tr}(\mathbf{D}\,\mathbf{B})\;\mathbf{B} + 2\,\mu\,\mathbf{D}, \tag{2.5}$$

where $\dot{\boldsymbol{\tau}}_e = (\partial\boldsymbol{\tau}_e/\partial t) + \mathbf{v}\cdot\boldsymbol{\nabla}\boldsymbol{\tau}_e$ denotes the material time derivative of the tensor $\boldsymbol{\tau}_e$. For the more general elastic behavior given by (2.2), corresponding expressions for the evolution of the extra stress may be found in the work of Bernstein (1960).

The simplest possible choice for the elastic behavior of the particles is of course the neo-Hookean model with $g(I) = \frac{\mu}{2}(I - 3)$. However, this model is unrealistic at large stretches for most materials, including elastomers, as it ignores the significant stiffening that such materials exhibit at large stretches. For this reason, in the applications to be

considered below, we will make use of the *Gent* model (Gent 1996), characterized by the choice

$$g(I) = -\frac{J_m\,\mu}{2}\ln\left(1-\frac{I-3}{J_m}\right), \tag{2.6}$$

where the dimensionless parameter $J_m > 0$, known as the *strain-locking* parameter, corresponds to the limiting value of $I-3$ at which the elastomer locks up (and the argument of the logarithm vanishes). Note that the Gent model (2.6) reduces to the neo-Hookean model in the limit as $J_m \to \infty$. The corresponding specialization of the constitutive relation (2.3) can then be written as

$$\boldsymbol{\tau}_e = \mu\left[\left(1-\frac{I-3}{J_m}\right)^{-1}\mathbf{B}-\mathbf{I}\right], \tag{2.7}$$

which in turn leads to the following evolution equation for the elastic extra stress tensor

$$\overset{\triangledown}{\boldsymbol{\tau}}_e = 2\,\mu\,\mathbf{D} + \frac{2}{\mu\,J_m}\mathrm{tr}\left[\mathbf{D}\left(\boldsymbol{\tau}_e+\mu\mathbf{I}\right)\right]\left(\boldsymbol{\tau}_e+\mu\mathbf{I}\right), \tag{2.8}$$

where use has been made of (2.7) to express $\mathbf{B}$ in terms of $\boldsymbol{\tau}_e$. Note that these expressions reduce to the well-known neo-Hookean expressions (Joseph 1990) in the limit as $J_m \to \infty$, namely,

$$\boldsymbol{\tau}_e = \mu(\mathbf{B}-\mathbf{I}), \quad \text{and} \quad \overset{\triangledown}{\boldsymbol{\tau}}_e = 2\,\mu\,\mathbf{D}. \tag{2.9}$$

Going back to the general expressions for the KV material, the viscous part of the extra stress can likewise be described in terms of a dissipation potential ϕ, which, on account of incompressibility and frame invariance, is a function of the last two invariants of $\mathbf{D}$, via

$$\boldsymbol{\tau}_v = \frac{\partial\phi(\mathbf{D})}{\partial\mathbf{D}}, \quad \mathrm{tr}(\mathbf{D}) = 0. \tag{2.10}$$

Although more general nonlinear forms could be considered, in this work, again for simplicity, we will focus our attention on linearly viscous behavior, such that

$$\boldsymbol{\tau}_v = 2\,\eta^{(2)}\,\mathbf{D}, \tag{2.11}$$

where $\eta^{(2)}$ describes the constant viscosity of the particle material.

It should be noted that the set of constitutive relations for KV particles reduces to those for purely elastic particles by taking the limit as the viscosity $\eta^{(2)}$ goes to zero. In this limit, the KV model simplifies to a hyperelastic model characterized by the stored-energy function $\psi(\mathbf{F})$. In other words, in this limit, the viscous part of the stress vanishes ($\boldsymbol{\tau}_v = \mathbf{0}$) and the elastic part coincides with the total stress ($\boldsymbol{\tau}_e = \boldsymbol{\tau}$). Therefore, for the case of (incompressible) Gent particles, the constitutive relation for the extra stress tensor ($\boldsymbol{\tau}$) and its evolution ($\overset{\triangledown}{\boldsymbol{\tau}}$) are given by (2.7) and (2.8), respectively, with $\boldsymbol{\tau}_e$ being replaced by $\boldsymbol{\tau}$. These relations have been shown to provide good agreement with experimental data for rubber-like materials (Ogden *et al.* 2004). Similarly, for the case of neo-Hookean particles, the corresponding relations are given by (2.9) with $\boldsymbol{\tau}_e$ being replaced by $\boldsymbol{\tau}$. In addition, it should be noted that the constitutive relations for KV particles also reduce to those for purely viscous (Newtonian) particles by taking the limit as the shear modulus μ tends to zero. However, our main interest in this work is on "solid" particles and we shall not consider this limit here, which would be more relevant for "fluid" inclusions (droplets) in the context of emulsions.

The suspending fluid (or the matrix) will be assumed here to be an incompressible

Newtonian fluid, with constitutive relation given by expression (2.1) with

$$\boldsymbol{\tau} = \boldsymbol{\tau}_v = 2\,\eta^{(1)}\,\mathbf{D}, \quad \mathrm{tr}(\mathbf{D}) = 0. \tag{2.12}$$

In other words, the constitutive behavior of the matrix will be taken to be purely viscous with linear response and constant viscosity $\eta^{(1)}$.

2.2. *Microstructures*

In this paper, we confine our attention to suspensions consisting of initially spherical, highly deformable, viscoelastic, solid particles that are distributed isotropically in a Newtonian viscous fluid (matrix). Based on earlier theoretical work for *dilute* concentrations of (non-interacting) deformable particles (Goddard & Miller 1967; Roscoe 1967; Gao *et al.* 2011, 2013), the particles are expected to change their shape and orientation when subjected to a shear flow. As already mentioned, for *dilute* concentrations, the initial spherical particles become aligned ellipsoids with a shape and orientation that evolves with the deformation until (possibly) reaching a steady state. On the other hand, for *non-dilute* concentrations (see the numerical simulations of Clausen *et al.* 2011, for moderately concentrated suspensions of capsules), it may be expected that the shape assumed by the viscoelastic particles in our suspensions will not be precisely ellipsoidal—deviations would be expected due to the non-uniform deformation fields that would be generated inside the particles as a consequence of the particle interactions. In addition, it would be expected that the shape and orientation of all the particles in the suspension would not be precisely the same, due to differences in the local environments "seen" by different particles. Nevertheless, in the spirit of generating simplified (homogenized) constitutive models for the instantaneous response of the non-dilute suspensions, as well as for the evolution of their microstructure, it makes sense to define suitable homogenized microstructural variables serving to characterize the evolution of the "average" shape and orientation of the particles, as functions of the deformation. Similarly, the two- and higher-point correlation functions for the distribution of the particle centers would be expected to evolve in a complicated way with the deformation. However, once again in the spirit of developing homogenized rheological models, it is reasonable to make use of simplified assumptions for the evolution of such correlation functions.

In the context of purely viscous systems, and ignoring surface tension effects (i.e., distributions of viscous drops in a viscous fluid), Kailasam & Ponte Castañeda (1998) proposed such a model utilizing a suitable application/generalization of the homogenization estimates of Ponte Castañeda & Willis (1995) for the "macroscopic" viscosity, as well as for the "average" strain rate and vorticity fields in the particle phase, to generate corresponding estimates for the instantaneous response of the suspension, as well as evolution laws for suitable microstructural variables characterizing the average shape and orientation of the particles, and of the two-point correlation functions describing the relative positions of the particles in the flow. In this context, it should be emphasized that the homogenization estimates of Ponte Castañeda & Willis (1995) provide a generalization of the dilute estimates of Eshelby (1957) for non-dilute dispersions of elastic particles in an elastic matrix (with different elastic moduli)—which can be reinterpreted for viscous particles in a viscous matrix—accounting for general ellipsoidal particle shapes distributed with generally different ellipsoidal shape for the two-point probability function for the particle-center distribution. The constitutive theory of Kailasam & Ponte Castañeda (1998) applies not only for linearly viscous behavior for the phases, but can also be used for nonlinearly viscous (including ideally plastic in the rate-independent limit) phases, and generalizes earlier work in this context by Kailasam *et al.* (1997) for the evolution of the particle shape and distribution (with fixed orientation). In this work,

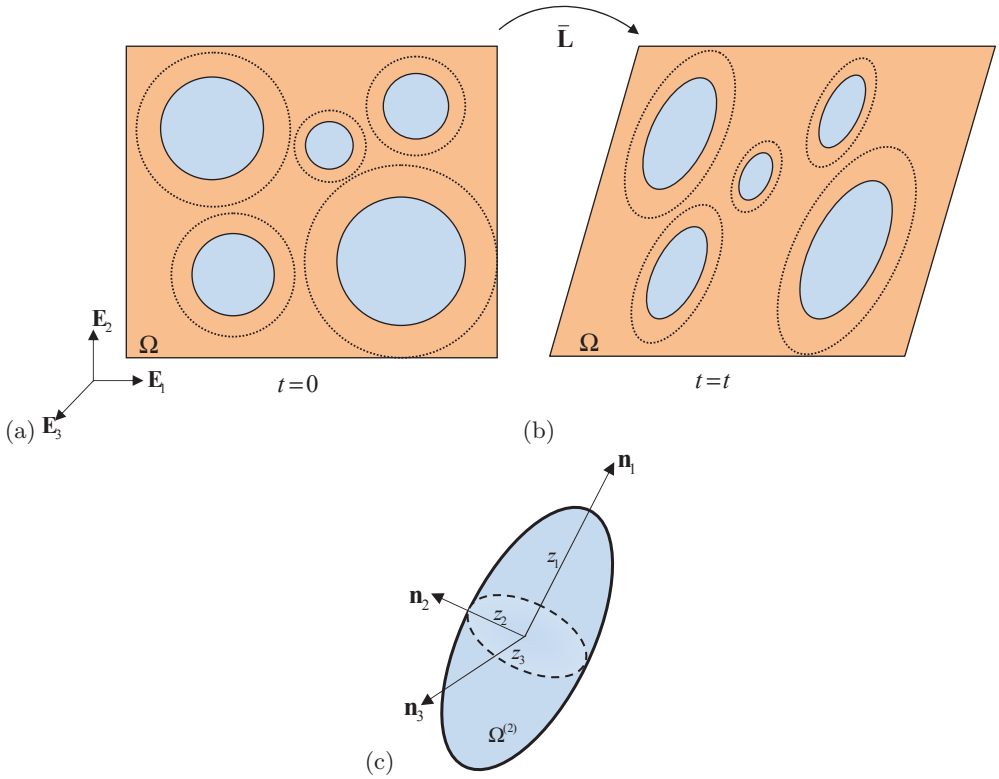

FIGURE 1. Schematic illustration of the microstructure in the suspension, identifying the various microstructural variables. The particles shapes and orientations evolve with the deformation and are depicted as grey ellipses, while their two-point probability functions are depicted as larger dotted ellipses surrounding the particles. (a) At $t = 0$, the particles are spherical and distributed randomly with statistical isotropy in the Newtonian fluid. (b) At a later time t, after application of the macroscopic velocity gradient $\bar{\mathbf{L}}$, the particles have become ellipsoidal and are distributed with ellipsoidal symmetry (with the same shape and orientation). (c) The particles are described by a "representative ellipsoid" with aspect ratios $w_1 = z_2/z_1$ and $w_2 = z_3/z_1$, and with principal axes defined by the unit vectors $\mathbf{n}_1$, $\mathbf{n}_2$ and $\mathbf{n}_3 = \mathbf{n}_1 \times \mathbf{n}_2$ (which rotate relative to the laboratory axes $\{\mathbf{E}_i\}$, $i = 1, 2, 3$.)

we propose a corresponding generalization of this theory to account for *viscoelastic* effects in the particles at *non-dilute* concentrations, building on the earlier work by Gao *et al.* (2011) for *dilute* concentration of *elastic* particles. This will require extending the notion of suitable microstructural variables to include the average elastic stress in the particles, as shall be seen in more detail further below.

Consistent with the just-stated objectives, we define next a special class of microstructures characterizing the *instantaneous* state of the system. Thus, it is assumed that at the present time all the initially (at zero time) spherical particles become ellipsoidal with identical shape and orientation as described by *representative* (average) ellipsoids

$$\Omega^{(2)} = \left\{ \mathbf{x} : |(\mathbf{Z})^{-T}\mathbf{x}| \leq 1 \right\}, \tag{2.13}$$

where $\mathbf{Z}$ is the so-called shape tensor. In addition, it will be assumed here that the relative position of the particles is described by two-point correlation functions having "ellipsoidal" symmetry. This notion was introduced by Willis (1977) to describe the shape for the angular dependence of two-point correlation functions, thus generalizing the notion of "statistical isotropy," which corresponds to spherical angular dependence. It

was used in the work of Ponte Castañeda & Willis (1995) to describe the shape of the two-point probabilities for the distribution of the centers of ellipsoidal particles with possibly different shapes and orientations, thus resulting in estimates depending on two *generally different* Eshelby-type microstructural tensors, one describing the shape and orientation of the particles and the other that of their distribution. While in general it may be expected that the shape and orientation of the particle distribution will evolve differently from the shape and orientation of the particles themselves, in this first investigation of the problem, we will assume, for simplicity, that the shape and orientation of the distribution functions is identical to that of the individual particles. We expect this to be a reasonable approximation for small to moderate particle volume fractions for two reasons. First, the effect of the particle distribution is expected to be of order volume fraction squared, while that of the particle themselves is expected to be of order volume fraction. Therefore, the effect of the shape of the distribution functions is expected to be small compared to that of the particle shapes themselves, at least for small to moderate volume fractions. Second, the numerical simulations of Clausen *et al.* (2011) for suspensions of concentrated capsules in a simple shear flow (see figures 11 and 13 in that paper) seem to suggest that this is not a bad approximation—certainly better than assuming that the distribution of the (non-Brownian) particles remains isotropic. Another possibility would be to assume that the shape and orientation of the particles evolves with the macroscopic deformation (Kailasam *et al.* 1997), as would be the case for periodic distributions of particles, but such an approximation would only be accurate for small enough volume fractions, and will not be pursued in this work, again mostly for simplicity, as it is much easier two work with one shape tensor than with two.

Figure 1(a) provides a schematic representation of the isotropic distribution of spherical particles in the suspension at $t = 0$. The spheres with solid and dotted lines represent cross sections of the particles and the distributional spheres, respectively. The triad $\{\mathbf{E}_i\}$, $(i = 1, 2, 3)$ is used to characterize the fixed laboratory coordinates. Figure 1(b) depicts a snapshot of the suitably idealized microstructure in the suspension at a future time instant t (recall that the particles and distributional ellipsoids are assumed to have the same shape and orientation at any moment). Also, Fig. 1(c) provides a schematic representation of the relevant microstructural variables at time t. The three orthonormal vectors $\mathbf{n}_1$, $\mathbf{n}_2$ and $\mathbf{n}_3 = \mathbf{n}_1 \times \mathbf{n}_2$ are used to characterize the principal axes of the particle. In this principal coordinate system, the shape tensor $\mathbf{Z}$ has the matrix representation $\mathbf{Z} = \mathrm{diag}(z_1, z_2, z_3)$ with z_1, z_2, z_3 being the three principal semi-axes of the ellipsoid. For future reference, it is convenient to define two aspect ratios

$$w_1 = z_2/z_1 \quad \text{and} \quad w_2 = z_3/z_1, \tag{2.14}$$

which fully characterize the shape of the particle.

Consistent with the above-described microstructural model, we choose the following set of variables to characterize the state of the ellipsoidal microstructure:

$$\mathscr{S} = \{w_1, w_2, \mathbf{n}_1, \mathbf{n}_2, \mathbf{n}_3 = \mathbf{n}_1 \times \mathbf{n}_2\}. \tag{2.15}$$

3. Macroscopic response

The objective of this section is to determine macroscopic constitutive relations for the rheological behavior of the suspensions described in the preceding section. As we have seen, we expect the mixture to go through a sequence of microstructures, approximately consisting of aligned ellipsoids that are distributed with ellipsoidal two-point statistics (with the same shape and orientation), which evolve in time, starting from an initial

state. In this work, we therefore break up the analysis of the macroscopic behavior of the suspensions into two parts. In the first, we assume that at a given instant the microstructure is specified, and make use of this information to estimate the *instantaneous* response of the mixture by means of a homogenization approach. In the second, we derive consistent *evolution* equations for the relevant microstructural variables making use of the corresponding instantaneous homogenization estimates for the average deformation and stress fields in the particles.

3.1. *Homogenization estimates for the instantaneous response*

We consider a *representative volume element* (RVE) of the suspension, which occupies a volume Ω with boundary $\partial\Omega$. The fluid and particle phases are in turn assumed to occupy volumes $\Omega^{(1)}$ and $\Omega^{(2)}$, respectively, such that $\Omega = \Omega^{(1)} + \Omega^{(2)}$. It is assumed that the RVE satisfies the *separation of length scales* hypothesis implying that the typical size of the neutrally buoyant particles is much smaller than the size of the RVE, as well as the Stokes condition in the fluid phase, such that

$$Re = \frac{\rho^{(1)}\,\dot{\gamma}\,d_p^2}{\eta^{(1)}} \to 0, \tag{3.1}$$

where $\rho^{(1)}$ is the density of the fluid, $\dot{\gamma}$ is a measure of the macroscopic strain rate and d_p is a measure of the particle diameter. Noting that the microstructure of the RVE is *statistically* uniform, a uniform *macroscopic* stress field will be generated in the RVE when an *affine* velocity boundary condition is applied on the boundary of the RVE ($\partial\Omega$). Thus, the suspension is subjected to the boundary condition

$$\mathbf{v}(\mathbf{x}) = \bar{\mathbf{L}}\mathbf{x}, \quad \text{on } \partial\Omega, \tag{3.2}$$

where $\bar{\mathbf{L}}$ ($\operatorname{tr}\bar{\mathbf{L}} = 0$) is the macroscopic, or average velocity gradient, defined by

$$\bar{\mathbf{L}} = \frac{1}{\operatorname{Vol}(\Omega)}\int_{\Omega} \mathbf{L}\,\mathrm{d}V. \tag{3.3}$$

(This follows from the *mean value theorem for the strain rate*, e.g., Ponte Castañeda & Suquet, 1998, which states that the volume average of the local strain-rate tensor $\mathbf{L}$ over the RVE under the affine velocity boundary condition (3.2) is precisely $\bar{\mathbf{L}}$.) Similarly, the average or macroscopic Cauchy stress is defined as

$$\bar{\boldsymbol{\sigma}} = \frac{1}{\operatorname{Vol}(\Omega)}\int_{\Omega} \boldsymbol{\sigma}\,\mathrm{d}V, \tag{3.4}$$

and the instantaneous macroscopic constitutive response is determined by the relation between $\bar{\boldsymbol{\sigma}}$ and $\bar{\mathbf{L}}$.

For future reference, we also define the phase averages of the strain-rate field over phase r ($r = 1, 2$) via

$$\bar{\mathbf{D}}^{(r)} = \frac{1}{\operatorname{Vol}(\Omega^{(r)})}\int_{\Omega^{(r)}} \mathbf{D}\,\mathrm{d}V, \tag{3.5}$$

such that

$$\bar{\mathbf{D}} = c^{(1)}\bar{\mathbf{D}}^{(1)} + c^{(2)}\,\bar{\mathbf{D}}^{(2)}, \tag{3.6}$$

with the $c^{(1)}$ and $c^{(2)}$ denoting the volume fractions of fluid and particle phases, respectively. Similarly, defining $\bar{\boldsymbol{\tau}}^{(1)}$ and $\bar{\boldsymbol{\tau}}^{(2)}$ as the averages of the extra stress in the fluid and particle phases, respectively, the macroscopic stress, as defined by (3.4), can be rewritten

(on account of the incompressibility of the phases) as

$$\bar{\boldsymbol{\sigma}} = -\bar{p}_0\,\mathbf{I} + c^{(1)}\,\bar{\boldsymbol{\tau}}^{(1)} + c^{(2)}\,\bar{\boldsymbol{\tau}}^{(2)}, \tag{3.7}$$

where $\bar{p}_0$ is an indeterminate hydrostatic pressure associated with the overall incompressibility of the suspension. Note that the effect of the compressibility of the bulk fluid has been considered by Brady *et al.* (2006) in the context of suspensions of rigid spherical particles.

Now, taking advantage of the special form of the constitutive relations for the fluid matrix and solid particle phases, as described in Section 2.1, *pseudo*-dissipation potentials are introduced

$$W^{(r)}(\mathbf{D}) = \eta^{(r)}\mathbf{D}\cdot\mathbf{D} + \boldsymbol{\tau}_e\cdot\mathbf{D}, \quad \mathrm{tr}(\mathbf{D}) = \mathbf{0}, \tag{3.8}$$

such that the local constitutive relation of the phases can be written as

$$\boldsymbol{\sigma} = -p_0\,\mathbf{I} + \boldsymbol{\tau}, \quad \text{where} \quad \boldsymbol{\tau} = \frac{\partial W^{(r)}}{\partial \mathbf{D}} = 2\,\eta^{(r)}\mathbf{D} + \boldsymbol{\tau}_e, \tag{3.9}$$

where p_0 is an indeterminate hydrostatic pressure. It should also be emphasized that the elastic strains $\boldsymbol{\tau}_e$ are considered to be fixed in taking the derivative with respect to $\mathbf{D}$. Thus, it can be seen that the addition of the linear term in the strain-rate tensor $\mathbf{D}$ to the dissipation function ϕ, defined by equation (2.10), allows the inclusion of the elastic stress $\boldsymbol{\tau}_e$, assuming that it is known at the given instant. More specifically, labeling the quantities associated with the matrix and particle phases by the superscripts (1) and (2), respectively, the local constitutive relation (3.9) can be used to recover the constitutive relations for the elastic particles and fluid matrix phases, as given by (2.1) to (2.12), provided that we let $\eta^{(1)}$ and $\eta^{(2)}$ be the viscosities of the fluid and elastic particles, respectively, and that we let $\boldsymbol{\tau}_e = 0$ in the fluid phase and $\boldsymbol{\tau}_e = \boldsymbol{\tau}_e^{(2)}$, as characterized by the evolution equation (2.8), in the particle phase. In addition, in this last expression, we use μ and J_m to describe the ground shear modulus and strain-locking parameter of the elastic particles, the subscript (2) having been dropped from μ and J_m for convenience (since only the particle phase has elastic properties, thus eliminating the risk of confusion).

We define next, for compactness, the local *pseudo*-dissipation potential

$$W(\mathbf{x},\mathbf{D}) = \chi^{(1)}(\mathbf{x})W^{(1)}(\mathbf{D}) + \chi^{(2)}(\mathbf{x})W^{(2)}(\mathbf{D}), \tag{3.10}$$

where the $\chi^{(r)}(\mathbf{x})$ ($r = 1, 2$) are the characteristic functions of the two phases, such that they are equal to one if the position vector $\mathbf{x}$ is in phase r (i.e., $\mathbf{x} \in \Omega^{(r)}$) and zero otherwise. Then, we can state the principle of minimum dissipation (see Keller *et al.* 1967) via

$$\min_{\mathbf{D}\in K} \int_{\Omega} W(\mathbf{x},\mathbf{D})\,\mathrm{d}V, \tag{3.11}$$

where K denotes the set of kinematically admissible strain rates:

$$K = \{\mathbf{D}|\ \text{there is}\,\mathbf{v}\,\text{such that}\,\mathbf{D} = (\nabla\mathbf{v} + (\nabla\mathbf{v})^T)/2\,,\mathrm{div}\,\mathbf{v} = 0\ \text{in}\ \Omega,\ \text{and}\,\mathbf{v} = \bar{\mathbf{L}}\mathbf{x}\ \text{on}\ \partial\Omega\}. \tag{3.12}$$

It is noted (see Ekeland & Témam 1999, for the purely viscous problem) that the Euler-Lagrange equations of this variational principle are precisely the Stokes equations for the fluid phase

$$2\,\eta^{(1)}\nabla^2\mathbf{v} - \nabla p = \mathbf{0}, \quad \nabla\cdot\mathbf{v} = 0, \tag{3.13}$$

together with the equilibrium equations for the solid particles, which in Eulerian form

become

$$2\,\eta^{(2)}\nabla^2\mathbf{v} - \nabla p_0 + \nabla\cdot\boldsymbol{\tau}_e^{(2)} = \mathbf{0}, \quad \nabla\cdot\mathbf{v} = 0, \tag{3.14}$$

where once again the elastic extra stress $\boldsymbol{\tau}_e^{(2)}$ in the particles is assumed to be known at the present instant. Note that the variational principle also ensures continuity of the velocity $\mathbf{v}$ and traction components of the *total* stress $\boldsymbol{\sigma}$ across the particle-fluid boundaries, as well as satisfaction of the affine boundary condition (3.2).

Finally, it is noted that the dissipation functional in equation (3.11), evaluated at the minimum, defines a function of the macroscopic strain-rate $\bar{\mathbf{D}}$, as given by the symmetric part of the average velocity gradient $\bar{\mathbf{L}}$. When normalized by the volume of the RVE Ω, it can be shown (see, for example, Ponte Castañeda & Suquet 1998) that it provides a *pseudo*-dissipation potential for the macroscopic constitutive relation, in the sense that

$$\bar{\boldsymbol{\sigma}} = -\bar{p}_0\,\mathbf{I} + \bar{\boldsymbol{\tau}}, \quad \text{where} \quad \bar{\boldsymbol{\tau}} = \frac{\partial\widetilde{W}}{\partial\bar{\mathbf{D}}}, \tag{3.15}$$

and where $\bar{p}_0$ is the Lagrange multiplier associated with the macroscopic incompressibility constraint and

$$\widetilde{W}(\bar{\mathbf{D}}) = \min_{\mathbf{D}\in K}\frac{1}{\mathrm{Vol}(\Omega)}\int_{\Omega} W(\mathbf{x},\mathbf{D})\,\mathrm{d}V. \tag{3.16}$$

The homogenization problem defined by equations (3.15) and (3.16) for the *instantaneous* response of the viscoelastic composite characterized by (3.8)–(3.10) is *mathematically analogous* to the corresponding problem for an incompressible *thermoelastic* composite with "elastic moduli" $\eta^{(r)}$ and "thermal stresses" $\boldsymbol{\tau}_e$ (provided that the strain rate and velocity fields are identified with the "strain" and "displacement" fields, respectively). For the specific problem of interest here, the viscosities (moduli) $\eta^{(r)}$ are *uniform-per-phase*, and while the elastic stress (thermal stress) in the matrix phase is zero, the corresponding elastic stress (thermal stress) in the particle phase is not only non-vanishing, but in fact also non-uniform. More general situations, including the case of nonuniform thermal stresses in the matrix phase has been considered recently by Lahellec *et al.* (2011).

To estimate the effective dissipation function $\widetilde{W}(\bar{\mathbf{D}})$, we make use of the Hashin-Shtrikman-Willis (HSW) variational method, which was originally developed for isotropic linear-elastic composites by Hashin & Shtrikman (1963), and extended later for generally anisotropic linear-elastic composites by Willis (1977, 1981). For the particulate material systems of interest in this work consisting of random distributions of ellipsoidal inclusions in a given matrix, more explicit estimates have been given by Ponte Castañeda & Willis (1995) still making use of the HSW variational method. When applied to the above-described viscous systems, the key feature of this method is the use of a "polarization field" relative to a homogeneous "comparison fluid" (with viscosity η^0). By means of this subterfuge, it is possible to make use of simple, constant-per-phase trial fields for the stress polarization to obtain bounds and estimates for the effective response of the composite system, which only depend on the appropriate first- and second-order statistics of the microstructure (i.e., the volume fraction and average shape and orientation of the particles, as well as the "shape" and "orientation" of the two-point statistics for the particle centers). The application of the method of Ponte Castañeda & Willis (PCW) to the class of suspensions of "thermoelastic" particles of interest in this work was given by Ponte Castañeda (2005). For completeness, the adaptation of these results to the above-defined problem for suspensions of viscoelastic particles is given in Appendix A. In this

section, we will only provide the final results for the macroscopic response, as well as for the average strain-rate and vorticity fields in the particle phase.

Thus, the resulting variational estimate for the effective dissipation function $\widetilde{W}(\bar{\mathbf{D}})$ can be expressed as

$$\widetilde{W}(\bar{\mathbf{D}}) = \eta^{(1)}\bar{\mathbf{D}}\cdot\bar{\mathbf{D}} + c\left(\eta^{(2)}-\eta^{(1)}\right)\bar{\mathbf{D}}^{(2)}\cdot\bar{\mathbf{D}} + \frac{c}{2}\,\bar{\boldsymbol{\tau}}_e^{(2)}\cdot\left(\bar{\mathbf{D}}^{(2)}+\bar{\mathbf{D}}\right), \tag{3.17}$$

where

$$\bar{\mathbf{D}}^{(2)} = \left\{\mathbb{I} - 2\,(1-c)\left(\eta^{(1)}-\eta^{(2)}\right)\mathbb{P}\right\}^{-1}\left\{\bar{\mathbf{D}} - (1-c)\,\mathbb{P}\,\bar{\boldsymbol{\tau}}_e^{(2)}\right\} \tag{3.18}$$

is the corresponding estimate for the average strain-rate over the particles. In these expressions, it is recalled from Appendix A that $c = c^{(2)}$ is the volume fraction of the particle phase, $\bar{\boldsymbol{\tau}}_e^{(2)}$ is the average elastic stress in the particles, and $\mathbb{P}$ is a microstructural (Eshelby-type) tensor given by $(\mathrm{A}\,11)_1$.

For later reference, we note that the procedure also provides an estimate for the average vorticity tensor in the particle phase (see Appendix A), which is given by

$$\bar{\mathbf{W}}^{(2)} = \bar{\mathbf{W}} + (1-c)\,\mathbb{R}\,\left[2\left(\eta^{(1)}-\eta^{(2)}\right)\bar{\mathbf{D}}^{(2)} - \bar{\boldsymbol{\tau}}_e^{(2)}\right], \tag{3.19}$$

where $\mathbb{R}$ is the microstructural tensor defined by $(\mathrm{A}\,11)_2$.

Finally, the instantaneous macroscopic constitutive relation for the suspension of viscoelastic particles can be obtained from the estimate (3.17) for $\widetilde{W}(\bar{\mathbf{D}})$ by means of equation (3.15). However, given $\bar{\mathbf{D}}^{(2)}$ and $\bar{\boldsymbol{\tau}}_e^{(2)}$, it is simpler to make use of expression (3.6) to write the average extra stress in the matrix phase as

$$\bar{\boldsymbol{\tau}}^{(1)} = 2\,\eta^{(1)}\bar{\mathbf{D}}^{(1)} = 2\,\eta^{(1)}\,(1-c)^{-1}\left(\bar{\mathbf{D}} - c\,\bar{\mathbf{D}}^{(2)}\right). \tag{3.20}$$

Then, substituting this expression into expression (3.7) for the macroscopic stress, we arrive at

$$\bar{\boldsymbol{\sigma}} = -\bar{p}\,\mathbf{I} + 2\,\eta^{(1)}\bar{\mathbf{D}} + c\left(\bar{\boldsymbol{\tau}}^{(2)} - 2\,\eta^{(1)}\bar{\mathbf{D}}^{(2)}\right), \tag{3.21}$$

which, using $(3.9)_2$ to express the average extra stress over the inclusion phase in terms of the extra elastic stress over the particles, finally leads to

$$\bar{\boldsymbol{\sigma}} = -\bar{p}_0\,\mathbf{I} + 2\,\eta^{(1)}\bar{\mathbf{D}} + 2\,c\left(\eta^{(2)}-\eta^{(1)}\right)\bar{\mathbf{D}}^{(2)} + c\,\bar{\boldsymbol{\tau}}_e^{(2)}. \tag{3.22}$$

Thus, it can be seen that for given macroscopic strain rate $\bar{\mathbf{D}}$, particle volume fraction c, and viscosities $\eta^{(1)}$ and $\eta^{(2)}$, the macroscopic Cauchy stress tensor $\bar{\boldsymbol{\sigma}}$ may determined from expression (3.22), by means of expression (3.18) for $\bar{\mathbf{D}}^{(2)}$ in terms of the current values of the average of the extra stress tensor over the particle $\bar{\boldsymbol{\tau}}_e^{(2)}$, together with the current values of the average aspect ratio and orientation of the particles, as defined by expression (2.15). It should be emphasized that the above results reduce to the corresponding *exact* results of Gao *et al.* (2011) for dilute concentrations ($c << 1$) and vanishing viscosity ($\eta^{(2)} = 0$) of the particles. (However, the results can also be shown to be exact for *dilute* concentrations of KV and other more general types of vicoelastic particles.) In the next subsection, we address the characterization of these variables by means of appropriate *evolution equations*, starting from an appropriate initial state where the particles are initially spherical and unstressed.

3.2. *Evolution equations for the microstructural variables and particle elastic stress*

So far, we have made use of Eulerian kinematics to describe the incremental behavior of the host fluid and particle phases, and accordingly generated estimates for the *in-*

stantaneous response of the suspension for a given state of the microstructure. However, when subjected to simple flows, the microstructure in the suspensions generally evolves in time as the applied deformation progresses. Therefore, in order to predict the effective *time-dependent* behavior of suspensions from a given initial state of the microstructure, it is crucial to first characterize the evolution of relevant microstructural variables. In addition, given that the instantaneous response depends on the current values of elastic stresses acting on the particles, which are determined by incremental constitutive equations of the type (2.8), it is also necessary to develop evolution laws for the average elastic stresses in the particles. As already anticipated in section 2.2, the initially spherical particles will deform—on average— through a sequence of ellipsoidal shapes throughout the deformation process. The average shape and orientation of the particles will be determined by standard kinematic arguments from expressions (3.18) and (3.19) for the instantaneous values of the average strain-rate and vorticity in the inclusion phase. In this connection, it is important to emphasize that the above expressions for the instantaneous average strain rate and vorticity inside particles will continue to apply at each increment of time, except that at each step the current values of the microstructural variables and of the elastic stresses in the particles will need to be used. It is also recalled from section 2.2 that, for simplicity, the "shape" and "orientation" of the angular dependence of the two-point correlation functions for the distribution of the particle centers will be assumed in this first work to be identical to the average shape and orientation of the particles themselves. As already mentioned, this reduces the number of microstructural variables required, and results in considerable simplification of the constitutive model.

First, recalling that the fluid and particle phases have been assumed to be incompressible, it follows that the volume fraction of the particles will remain constant throughout any deformation process, *i.e.*,

$$c = const. \tag{3.23}$$

On the other hand, the evolution for the particle aspect ratios w_1 and w_2, as defined by (2.14), are obtained by identifying the rate of change of the stretch of the particles along its principal axes with the appropriate normal components of the average strain-rate tensor in the particles, such that (see, for example, Bilby & Kolbuszewski 1977)

$$\dot{w}_1 = w_1(\bar{D}^{(2)}_{22} - \bar{D}^{(2)}_{11}), \qquad \dot{w}_2 = w_2(\bar{D}^{(2)}_{33} - \bar{D}^{(2)}_{11}), \tag{3.24}$$

where it is noted that the overdot here denotes simple time derivatives (since w_1 and w_2 depend only on time). It is also remarked in this context that the components of the tensorial variables associated with the particle phase, here and elsewhere, are referred to the principal axes of the ellipsoidal particle in their current state, as given by the triad $\{\mathbf{n}_1, \mathbf{n}_2, \mathbf{n}_3\}$.

Next, the evolution of the orthonormal vectors $\mathbf{n}_1$, $\mathbf{n}_2$ and $\mathbf{n}_3$, serving to characterize the orientation of particles, are determined by means of the kinematical relations

$$\dot{\mathbf{n}}_i = \mathbf{\Omega}\,\mathbf{n}_i, \qquad i = 1, 2, 3, \tag{3.25}$$

where $\mathbf{\Omega}$ is the (antisymmetric) spin tensor of the particle, whose components in the principal coordinate system $\{\mathbf{n}_1, \mathbf{n}_2, \mathbf{n}_3\}$ are determined in terms of the average strain rate and vorticity in the particles by means of the following relations (Kailasam & Ponte Castañeda 1998; Aravas & Ponte Castañeda 2004)

$$\Omega_{ij} = \bar{W}^{(2)}_{ij} - \frac{(w_{i-1})^2 + (w_{j-1})^2}{(w_{i-1})^2 - (w_{j-1})^2}\,\bar{D}^{(2)}_{ij}, \qquad i \neq j. \tag{3.26}$$

In this notation, when i or j is equal to 1, we define $w_{1-1} = w_0 = 1$. It should also be noted that alternative expressions for the evolution of the microstructure can be derived directly in terms of the particle shape tensors $\mathbf{Z}$, as shown by Goddard & Miller (1967).

As can be seen from relations (3.22), together with (3.18), the calculation of the instantaneous macroscopic stress in the suspension requires knowledge of the average elastic extra stress in the particle phase. As discussed in Appendix A, due to the choice of *constant-per-phase* polarization fields, together with the choice of $\eta^0 = \eta^{(1)}$, the PCW homogenization theory results in uniform stress and strain fields in the particle phase. As a consequence of this result, the constitutive relations for the average elastic stress fields in the particle phase take the same form as in the corresponding relations for the local fields. Therefore, for the case of KV particles with a Gent-type elastic stress (characterized by relations (2.7) and (2.8)), the evolution equations for the average elastic extra stress in the particles is given by

$$\begin{aligned}\overset{\nabla}{\bar{\boldsymbol{\tau}}}{}_e^{(2)} &= \dot{\bar{\boldsymbol{\tau}}}_e^{(2)} - \bar{\mathbf{L}}^{(2)}\bar{\boldsymbol{\tau}}_e^{(2)} - \bar{\boldsymbol{\tau}}_e^{(2)}(\bar{\mathbf{L}}^{(2)})^T \\ &= 2\,\mu\,\bar{\mathbf{D}}^{(2)} + \frac{2}{\mu\,J_m}\mathrm{tr}\left[\bar{\mathbf{D}}^{(2)}\left(\bar{\boldsymbol{\tau}}_e^{(2)} + \mu\mathbf{I}\right)\right]\left(\bar{\boldsymbol{\tau}}_e^{(2)} + \mu\mathbf{I}\right), \end{aligned} \tag{3.27}$$

where the material time derivative $\dot{\bar{\boldsymbol{\tau}}}_e^{(2)}$ appearing in the above expression is a simple, time derivative, due to the fact that the stress field inside the particle is uniform (as already mentioned) and the convective terms hence vanish. Note that the corresponding "integral" form of the constitutive equation is given by

$$\bar{\boldsymbol{\tau}}_e^{(2)} = \mu\left[\left(1 - \frac{\bar{I}^{(2)} - 3}{J_m}\right)^{-1}\bar{\mathbf{B}}^{(2)} - \mathbf{I}\right], \quad \bar{\boldsymbol{\tau}}_v^{(2)} = 2\,\eta^{(2)}\,\bar{\mathbf{D}}^{(2)}. \tag{3.28}$$

where $\bar{I}^{(2)} = \mathrm{tr}(\bar{\mathbf{B}}^{(2)})$, $\bar{\mathbf{B}}^{(2)} = \bar{\mathbf{F}}^{(2)}(\bar{\mathbf{F}}^{(2)})^T$ and $\bar{\mathbf{F}}^{(2)}$ is the average deformation gradient in the particles.

It should also be noted that, in the limit as $J_m \to \infty$ (corresponding to KV particles with a neo-Hookean elastic part), the above evolution equation simplifies to

$$\overset{\nabla}{\bar{\boldsymbol{\tau}}}{}_e^{(2)} = 2\,\mu\,\bar{\mathbf{D}}^{(2)}. \tag{3.29}$$

In summary, for a given macroscopic velocity gradient $\bar{\mathbf{L}} = \bar{\mathbf{D}} + \bar{\mathbf{W}}$, the macroscopic stress $\bar{\boldsymbol{\sigma}}$ in the suspension is given by expression (3.22), where $\bar{\mathbf{D}}^{(2)}$ is given by expression (3.18). These quantities depend on the particle volume fraction c, and on the current values of the microstructural variables $\mathscr{S}$, as defined by expression (2.15), and determined by the evolution equations (3.24) and (3.25) from some known initial state, as well as on the current value of the average extra elastic stress $\bar{\boldsymbol{\tau}}_e^{(2)}$ in the particles, as determined by expression (3.27). Note that the evolution equation for the particle axes (3.25) involves the average vorticity tensor in the particles, which is given in terms of other "known" variables at the given time instant by expression (3.19). Due to the complex dependence of the microstructural tensors $\mathbb{P}$ and $\mathbb{R}$ on the microstructural variables $\mathscr{S}$, it is not possible to simplify further these expressions in general.

In the context of the above-developed rheological model for dispersions of viscoelastic solid particles, it is important to emphasize that although the exact solution for the fields in the particles is not uniform in general, the uniform-field approximation in the inclusion phase is *exact* for dilute concentrations of particles ($c << 1$), as originally argued by Roscoe (1967) for the steady-state solutions (when available), and shown by Gao *et al.* (2011) for more general time-dependent motions of dilute suspensions of purely elastic particles ($\eta^{(2)} = 0$). (The work of Gao *et al.* (2011) can be easily generalized

to consider more general types of viscoelastic behavior for the particles, including the Kevin-Voigt model used in this work.) For non-dilute concentrations of particles, it is expected that the approximation of uniform fields in the particles will lead to fairly accurate results for low to moderate concentrations. However, as already mentioned, although serving to provide bounds for both poly- and mono-disperse microstructures, the PCW-type estimates on which the model is based are more appropriate for poly-disperse microstructures. For these reasons, it would be expected that the domain of application of the above-developed model for suspensions of elastic particles would be larger for poly-disperse suspensions than for mono-disperse suspensions. For related reasons, the homogenization model cannot handle strong interaction effects among the particles, such as the formation of clusters, which would be expected for mono-disperse systems at fairly high concentrations. Finally, it should be remarked that in the limit as the shear modulus of the particles μ tends to zero, the constitutive model developed in the present work formally reduces to corresponding models developed by Kailasam & Ponte Castañeda (1998) for non-dilute dispersions of viscous particles (and, therefore also, to the results of Wetzel & Tucker 2001, for dilute dispersions of such particles). However, in spite of their theoretical interest, such models do not account for the effects of surface tension at the droplet-matrix interfaces, and as such cannot be used in practice as constitutive models for emulsions. In fact, the main objective of the work of Kailasam & Ponte Castañeda (1998) was to develop nonlinear constitutive models for the high-temperature creep (or high strain-rate flow) of two-phase metals or rocks, where the viscous response of the phases can be described by non-linear (power-law) constitutive laws, and interfacial tension can be neglected.

4. Steady-state estimates for the suspensions

It is known from earlier works (Roscoe 1967; Goddard & Miller 1967) that an initially spherical particle with Kelvin-Voigt viscoelastic behavior suspended in an infinite Newtonian fluid can admit, under certain conditions, steady-state (SS) solutions, where the particle becomes an ellipsoid with fixed shape and orientation, while undergoing tank-treading motion with constant stress, strain rate and vorticity. According to the theory developed in Section 3, the stress and strain-rate fields are (approximately) uniform inside the particle phase, and steady-state solutions should still be possible for non-dilute concentrations of initially spherical, viscoelastic particles. In this case, existence of a SS solution will depend on flow conditions, as well as on the constitutive properties and volume fraction of the particles. For definiteness, we note that all variables in this section are evaluated at the steady state.

The SS solutions, if they exist, can be determined by setting the terms involving time derivatives equal to zero in the evolution equations for the extra stress tensor inside the particle, as well as in the evolution equations for the particle shape and orientation. The resulting expressions provide a set of algebraic equations to be solved for the six components of the extra stress tensor in the particle, $\bar{\boldsymbol{\tau}}^{(2)}$, the two aspect ratios, ω_1, ω_2, and the three orientational angles defined by the particle axes, $\mathbf{n}_1$, $\mathbf{n}_2$, and $\mathbf{n}_3$.

First, making use of the incompressibility constraint in the particle phase ($\mathrm{tr}(\bar{\mathbf{D}}^{(2)}) = 0$), together with the evolution equation for the aspect ratios (3.24), we deduce that, at the steady state, the normal components of the strain-rate tensor in the particle phase, relative to the principal axes $\mathbf{n}_i$ of the ellipsoidal particles, are equal to zero:

$$\bar{D}^{(2)}_{11} = \bar{D}^{(2)}_{22} = \bar{D}^{(2)}_{33} = 0. \tag{4.1}$$

Also, at the steady state, the evolution equations for the particle orientation, given by

(3.25) and (3.26), imply that the three components of the vorticity tensor in the particle phase are given by

$$\bar{W}_{12}^{(2)} = \frac{1+w_1^2}{1-w_1^2}\bar{D}_{12}^{(2)}, \quad \bar{W}_{13}^{(2)} = \frac{1+w_2^2}{1-w_2^2}\bar{D}_{13}^{(2)}, \quad \bar{W}_{23}^{(2)} = \frac{w_1^2+w_2^2}{w_1^2-w_2^2}\bar{D}_{23}^{(2)}. \tag{4.2}$$

Next, recalling that the principal axes of the Finger tensor $\bar{\mathbf{B}}^{(2)} = (\bar{\mathbf{V}}^{(2)})^2$ correspond to the Eulerian axes of the deformation in the particles, so that the Eulerian axes coincide with the principal axes of the ellipsoidal particles, it follows that, at the steady state, when the particles have reached a fixed orientation, their orientation becomes fixed and is characterized by the triad $\{\mathbf{n}_1, \mathbf{n}_2, \mathbf{n}_3\}$. This implies that, at the steady-state solution, the shear components of the Finger tensor (relative to the particle axes) must all vanish:

$$\bar{B}_{12}^{(2)} = \bar{B}_{13}^{(2)} = \bar{B}_{23}^{(2)} = 0. \tag{4.3}$$

Moreover, the normal components of $\bar{\mathbf{B}}^{(2)} = (\bar{\mathbf{V}}^{(2)})^2$ (again, relative to the particle axes) correspond to the principal stretches of the deformation in the particles:

$$\bar{B}_{ii}^{(2)} = \left(\bar{\lambda}_i^{(2)}\right)^2, \quad i = 1,2,3 \quad \text{(no sum)}, \tag{4.4}$$

where $\bar{\lambda}_i^{(2)}$ $(i = 1,2,3)$ denote the principal stretches of the deformation in the particles, i.e., the principal values of the left stretch tensor $\bar{\mathbf{V}}^{(2)}$ in the particle. On the other hand, the shape of the particle is described by the principal stretches as (see Figure 1(c) for definitions of w_1 and w_2)

$$w_1 = \bar{\lambda}_2^{(2)}/\bar{\lambda}_1^{(2)}, \quad w_2 = \bar{\lambda}_3^{(2)}/\bar{\lambda}_1^{(2)}, \tag{4.5}$$

Making use of the above relations in (4.4), together with the incompressibility constraint in the particle phase ($\bar{J}^{(2)} = \det(\bar{\mathbf{F}}^{(2)}) = \bar{\lambda}_1^{(2)}\,\bar{\lambda}_2^{(2)}\,\bar{\lambda}_3^{(2)} = 1$), we find that

$$\bar{B}_{11}^{(2)} = (w_1\,w_2)^{-2/3}, \quad \bar{B}_{22}^{(2)} = (w_1)^{4/3}\,(w_2)^{-2/3}, \quad \bar{B}_{33}^{(2)} = (w_1)^{-2/3}\,(w_2)^{4/3}. \tag{4.6}$$

In this context, it is worth mentioning that the components of the tensor $\bar{\mathbf{B}}^{(2)}$ in relations (4.3) and (4.6) identically satisfy the evolution equation for the Finger tensor $\bar{\mathbf{B}}^{(2)}$ (i.e., $\overset{\nabla}{\bar{\mathbf{B}}}{}^{(2)} = \mathbf{0}$) at the steady-state solution. Finally, we emphasize that the kinematical equations (4.1)-(4.6) are valid at SS solutions (if they exist) regardless of the constitutive behavior of particles. In the following subsection, we outline the additional *constitutive* equations in SS solutions for the case of KV particles.

4.1. *Steady-state solution for Kelvin-Voigt particles*

In this subsection, we consider steady-state solutions in non-dilute suspensions of Kelvin-Voigt particles, characterized by constitutive equations (3.28). Making use of (4.3) in $(3.28)_1$, we find that the shear components of the elastic extra stress tensor (relative to the particle axes) are zero at the SS solution:

$$(\bar{\tau}_e^{(2)})_{12} = (\bar{\tau}_e^{(2)})_{13} = (\bar{\tau}_e^{(2)})_{23} = 0. \tag{4.7}$$

Similarly, we find the three remaining (normal) components of the elastic extra stress tensor by making use of (4.6) in the constitutive relation $(3.28)_1$. The final results read

as

$$
\begin{aligned}
(\bar{\tau}_e^{(2)})_{11} &= \mu\, d_w \left\{ J_m\, (w_2)^{1/3} \left[1 - (w_1\, w_2)^{2/3} \right] + c_w \right\}, \\
(\bar{\tau}_e^{(2)})_{22} &= \mu\, d_w \left\{ J_m\, (w_2)^{1/3} \left[(w_1)^2 - (w_1\, w_2)^{2/3} \right] + c_w \right\}, \\
(\bar{\tau}_e^{(2)})_{33} &= \mu\, d_w \left\{ J_m\, (w_2)^{1/3} \left[(w_2)^2 - (w_1\, w_2)^{2/3} \right] + c_w \right\},
\end{aligned}
\tag{4.8}
$$

where $c_w = (w_2)^{1/3} \left[(w_1)^2 + (w_2)^2 + 1 \right] - 3\, (w_1)^{2/3}\, w_2$, and $d_w = \left[J_m\, (w_1)^{2/3}\, w_2 - c_w \right]^{-1}$. In the limit as $J_m \to \infty$ (corresponding to KV particles with neo-Hookean elastic behavior), relations (4.8) simplify to

$$
\begin{aligned}
&(\bar{\tau}_e^{(2)})_{11} = \mu \left[(w_1\, w_2)^{-2/3} - 1 \right], \quad (\bar{\tau}_e^{(2)})_{22} = \mu \left[(w_1)^{4/3}\, (w_2)^{-2/3} - 1 \right], \\
&(\bar{\tau}_e^{(2)})_{33} = \mu \left[(w_1)^{-2/3}\, (w_2)^{4/3} - 1 \right].
\end{aligned}
\tag{4.9}
$$

Now, making use of (4.7) in (3.18) and (3.19), the non-zero components of the particle strain-rate $\bar{\mathbf{D}}^{(2)}$ and vorticity $\bar{\mathbf{W}}^{(2)}$ at the steady state can be written as

$$
\bar{D}_{ij}^{(2)} = \frac{\bar{D}_{ij}}{1 - \alpha\, \mathbb{P}_{ijij}}, \quad \bar{W}_{ij}^{(2)} = \bar{W}_{ij} + \frac{\alpha\, \mathbb{R}_{ijij}\, \bar{D}_{ij}}{1 - \alpha\, \mathbb{P}_{ijij}}, \quad i,j = 1,2,3 \text{ (no sum, } i \neq j), \tag{4.10}
$$

where $\alpha = 4\,(1-c)\,(\eta^{(1)} - \eta^{(2)})$ and all components are given relative to the particle axes.

Next, relations (4.1) together with the constitutive equation $(3.28)_2$ imply that, at the steady state, the normal components of the viscous part of extra stress tensor (relative to the particle axes) in the KV particles must all vanish:

$$
(\bar{\tau}_v^{(2)})_{11} = (\bar{\tau}_v^{(2)})_{22} = (\bar{\tau}_v^{(2)})_{33} = 0. \tag{4.11}
$$

Moreover, substituting the shear components of $\bar{\mathbf{D}}^{(2)}$ from $(4.10)_1$ into $(3.28)_2$, we find the shear components of $\bar{\boldsymbol{\tau}}_v^{(2)}$ as follows

$$
(\bar{\tau}_v^{(2)})_{ij} = \frac{2\,\eta^{(2)}\, \bar{D}_{ij}}{1 - 4\,(1-c)\,(\eta^{(1)} - \eta^{(2)})\, \mathbb{P}_{ijij}}, \quad i,j = 1,2,3 \;\; (i \neq j). \tag{4.12}
$$

Finally, the components of the total extra stress tensor in the KV particles at the steady state can be obtained in terms of the above estimates for the viscous and elastic extra stresses in the particles by means of the relation

$$
\bar{\tau}_{ij}^{(2)} = (\bar{\tau}_e^{(2)})_{ij} + (\bar{\tau}_v^{(2)})_{ij}. \tag{4.13}
$$

At this stage, all non-zero components of the particle stress $\bar{\boldsymbol{\tau}}^{(2)}$, strain-rate $\bar{\mathbf{D}}^{(2)}$ and vorticity $\bar{\mathbf{W}}^{(2)}$ are written in terms of steady-sate values of the aspect ratios, w_1 and w_2, and the three orientational angle defined by the particles axes, $\mathbf{n}_1$, $\mathbf{n}_2$, and $\mathbf{n}_3$. Making use of (4.8) into (3.18), together with the three equations obtained by substituting relations (4.10) into (4.2), and expression (4.1), we obtain a system of algebraic equations for the unknowns $w_1, w_2, \mathbf{n}_1, \mathbf{n}_2, \mathbf{n}_3$.

In conclusion, it is important to remark that the SS solutions provided in this section generalize the work of Roscoe (1967) in two ways: (1) they extend the results of Roscoe to the finite concentration regime, (2) they apply for Kelvin-Voigt particles with more general elastic parts (Gent behavior), which allows these results to incorporate the dependence on the extensibility of the particles (through the parameter J_m). Indeed, in the limiting case of $c << 1$ and $J_m \to \infty$, the aforementioned system of equations, when applied for the cases of simple shear flow and extensional flow, will recover, respectively,

the system of equations (78)-(80) and equation (98) in Roscoe (1967), given for a dilute suspension of KV particles with neo-Hookean elastic response. (We emphasize, in this connection, that there is a typo in the RHS of equation (79) in Roscoe's paper: the plus sign should be replaced by a minus sign. This error can be verified by doing the pertinent algebra mentioned before equation (78) in that paper.)

We remark that the SS solutions for suspensions of KV particles reduce to those for suspensions of elastic particles by setting $(\bar{\tau}_e^{(2)})_{ij} = \bar{\tau}_{ij}^{(2)}$ and $(\bar{\tau}_v^{(2)})_{ij} = 0$ $(i, j = 1, 2, 3)$ in relations (4.7)-(4.13). For the special case of neo-Hookean particles, relations (4.9) agree exactly with the corresponding steady-state relations provided in Gao *et al.* (2011) for the normal components of the extra stress tensor (see relations (4.9) in the reference). In addition, in the limit as $c \to 0$, the above expressions reproduce exactly the corresponding exact estimates of Gao *et al.* (2011) for the particle aspect ratios and orientation angles for dilute concentration of particles.

5. Applications and discussion

With the objective of illustrating the physical implications of the constitutive model developed in Section 3, in this section we apply the model to suspensions of incompressible, viscoelastic particles in macroscopically uniform flows for representative volume fractions and constitutive properties of the particles. In particular, we consider suspensions of initially spherical particles in Newtonian fluids under two special types of flows: *extensional* and *shear* flows. For convenience, we make use of the dimensionless parameters

$$K = \frac{\eta^{(2)}}{\eta^{(1)}}, \quad \text{and} \quad G = \frac{\eta^{(1)}\,\dot{\gamma}}{\mu},$$

serving to characterize the particle-fluid viscosity ratio and the ratio of viscous forces in the fluid to the elastic forces in the particles, respectively.

5.1. *Suspensions of initially spherical particles in an extensional flow*

First, we consider suspensions of initially spherical particles in an extensional flow with

$$\bar{\mathbf{L}} = \bar{\mathbf{D}} = \dot{\gamma}\,\mathbf{E}_1 \otimes \mathbf{E}_1 - \frac{1}{2}\dot{\gamma}\,(\mathbf{E}_2 \otimes \mathbf{E}_2 + \mathbf{E}_3 \otimes \mathbf{E}_3)\,, \tag{5.1}$$

where the $\{\mathbf{E}_i\}$ refer to the fixed laboratory coordinate system and $\dot{\gamma} > 0$ is the macroscopic strain rate. Because of the symmetry of the flow, as well as the incompressibility of the particles in the suspension, the particles do not rotate and the only microstructural parameter which evolves under the flow is the aspect ratio of the (axi-symmetric) particles, $w = w_1 = w_2$. In this case the microstructural tensor $\mathbb{P}$ is explicit and we can derive correspondingly explicit expressions for the evolution of the aspect ratio w and the extra elastic stresses $\bar{\boldsymbol{\tau}}_e^{(2)}$ in the particles, as determined by (3.24) and (3.27), respectively. To maintain continuity, these equations are provided in Appendix B. Then, given the current values of the elastic stresses $\bar{\boldsymbol{\tau}}_e^{(2)}$ and the aspect ratio w of the particles, the macroscopic stress $\bar{\boldsymbol{\sigma}}$ can be derived by means of expression (3.22), together with (3.18).

For the purpose of efficiently describing the macroscopic response of the suspension in an extensional flow, it is useful to introduce the effective *extensional* viscosity of the suspensions via

$$\tilde{\eta}_E = \frac{3\,(\bar{\sigma}_{11} - \bar{\sigma}_{22})}{2\,(\bar{D}_{11} - \bar{D}_{22})} = \frac{1}{\dot{\gamma}}(\bar{\sigma}_{11} - \bar{\sigma}_{22}), \tag{5.2}$$

where the components of the relevant tensors are relative to the fixed laboratory axes

and use has been made of $\bar{\sigma}_{33} = \bar{\sigma}_{22}$ (which follows from the flow symmetry). Also, the corresponding *intrinsic* viscosity of the suspension is defined by

$$\tilde{\eta}'_E = \frac{1}{c}\left(\frac{\tilde{\eta}_E}{3\,\eta^{(1)}} - 1\right). \tag{5.3}$$

To obtain the initial viscosity of the suspension, we make use of the (initial) condition $\bar{\boldsymbol{\tau}}_e^{(2)}\Big|_{t=0} = \mathbf{0}$, which implies that, at $t = 0$, the suspension of KV particles behaves like a suspension of spherical viscous drops with viscosity ratio $K = \eta^{(2)}/\eta^{(1)}$. Therefore, making use of the corresponding estimates of Kailasam & Ponte Castañeda (1998) for suspensions of viscous drops (which ignore surface tension effects), the initial relative viscosity can be written as

$$\left.\frac{\tilde{\eta}_E}{3\,\eta^{(1)}}\right|_{t=0} = \frac{3\,(1-c) + (2+3c)\,K}{3 + 2\,c + 2\,(1-c)\,K}. \tag{5.4}$$

However, for the special case of purely elastic particles, the initial response of the suspension is like that of suspensions of incompressible voids ($K = 0$). Hence, in this case, the relative viscosity at $t = 0$ is given by

$$\left.\frac{\tilde{\eta}_E}{3\,\eta^{(1)}}\right|_{t=0} = \frac{3\,(1-c)}{3 + 2\,c}. \tag{5.5}$$

Figure 2 presents results for the time-dependent behavior of a suspension of purely elastic particles with $G = 0.3$ in extensional flow. Thus, figures 2(a) and (b) show respectively the results for the evolution of w for suspensions of NH particles at several values of the particle volume fraction, and for suspensions of Gent particles at the fixed volume fraction $c = 0.2$ and different values of the strain-locking parameter. We observe from figure 2(a) that the particle volume fraction has a critical effect on the transient elongation of the NH particles. In particular, we observe that, for higher values of c ($c = 0.15, 0.2$), the time-dependent deformation of NH particles never reaches a steady state, and instead the NH particles keep elongating. On the contrary, we observe from figure 2(b) that the time-dependent deformation of Gent particles with $c = 0.2$ reaches a steady state, except for the case of $J_m \to \infty$ which corresponds to NH particles. This is because the *inextensibility* constraint of the Gent particles with a finite value of J_m prevents the particles from deforming indefinitely under the applied flow. Although results are shown only for $c = 0.2$ for the Gent particles, as we will see later, the response of the Gent particles—unlike that of the NH particles—is qualitatively the same for all values of c. Next, figures 2(c) and (d) show corresponding results for the non-zero components of $\bar{\boldsymbol{\tau}}^{(2)}$, for the cases of NH and Gent particles, respectively. We observe from figure 2(c) that the continuous elongation of the NH particles for higher values of c leads to very high—eventually becoming unbounded—stresses in these particles along the extensional direction (i.e., $\mathbf{E}_1$-direction). On the other hand, as observed from figure 2(d) for the Gent particles with $c = 0.2$, all the stresses reach finite values (including for $J_m = 500$, although for stresses higher than shown in the figure). This is because the Gent particles—different from the NH particles—cannot continue to stretch indefinitely and therefore can no longer completely "block" the overall flow. Finally, figures 2(e) and (f) show corresponding results for the intrinsic viscosities $\tilde{\eta}'_E$ of the suspensions, for the cases of NH and Gent particles, respectively. For the case of NH particles (figures 2(e)), we see that the effective viscosity blows up for the higher values of c, which is a consequence of the unbounded stresses that develop in the NH particles. On the other hand, we observe from figure 2(f) that for the case of Gent particles (including those with

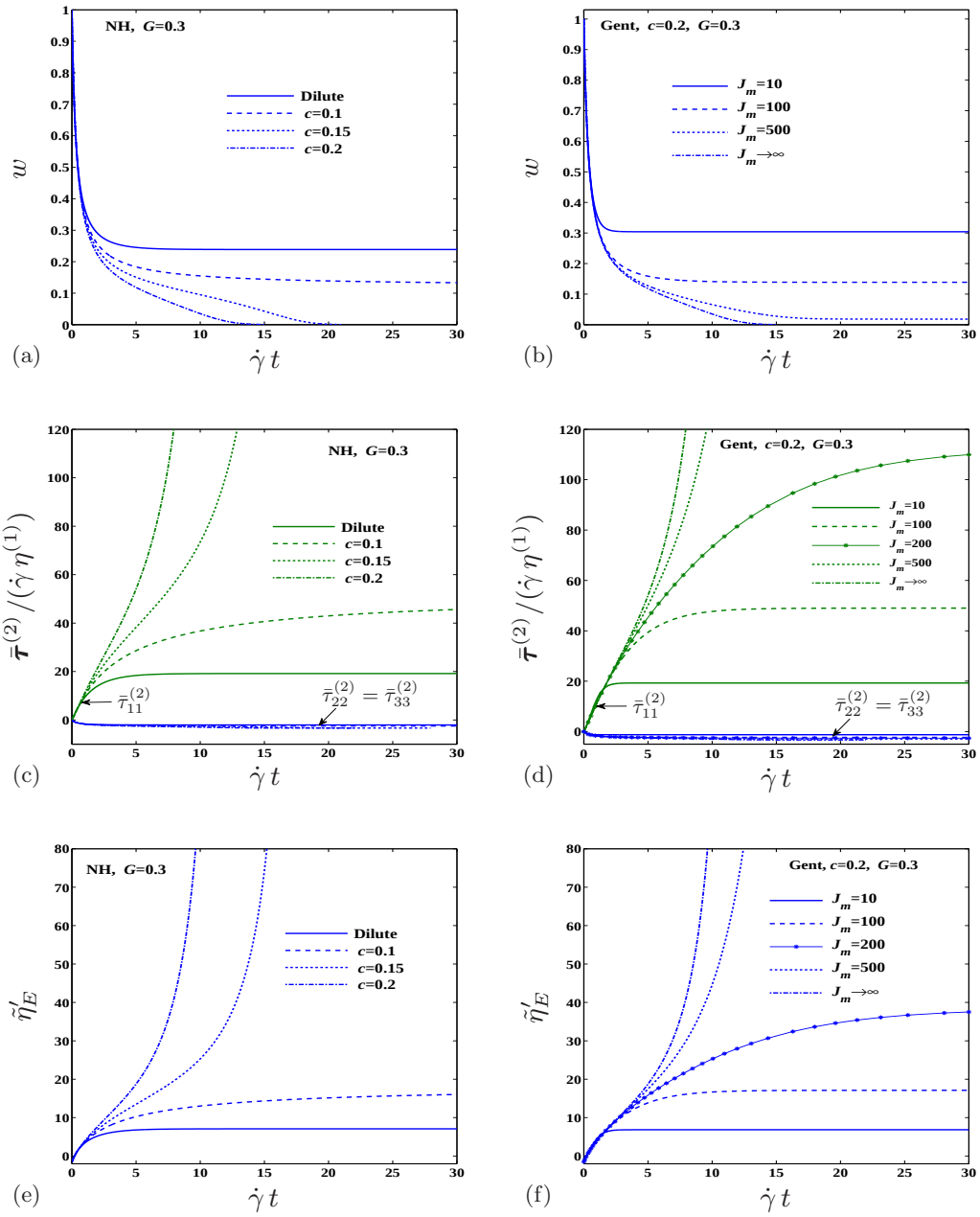

FIGURE 2. Results for the time-dependent response of suspensions of initially spherical neo-Hookean and Gent particles with $G = 0.3$ in an extensional flow. (a)-(b) Average aspect ratio of the particles. (c)-(d) Average extra stresses in the particles. (e)-(f) Intrinsic viscosity of the suspension.

$J_m = 500$, although not apparent from the plot), the effective viscosity always reaches *finite* SS values, such that the smaller the value of J_m, the smaller the SS value of the effective viscosity.

Figure 3 provides estimates for the time-dependent response of the suspensions of

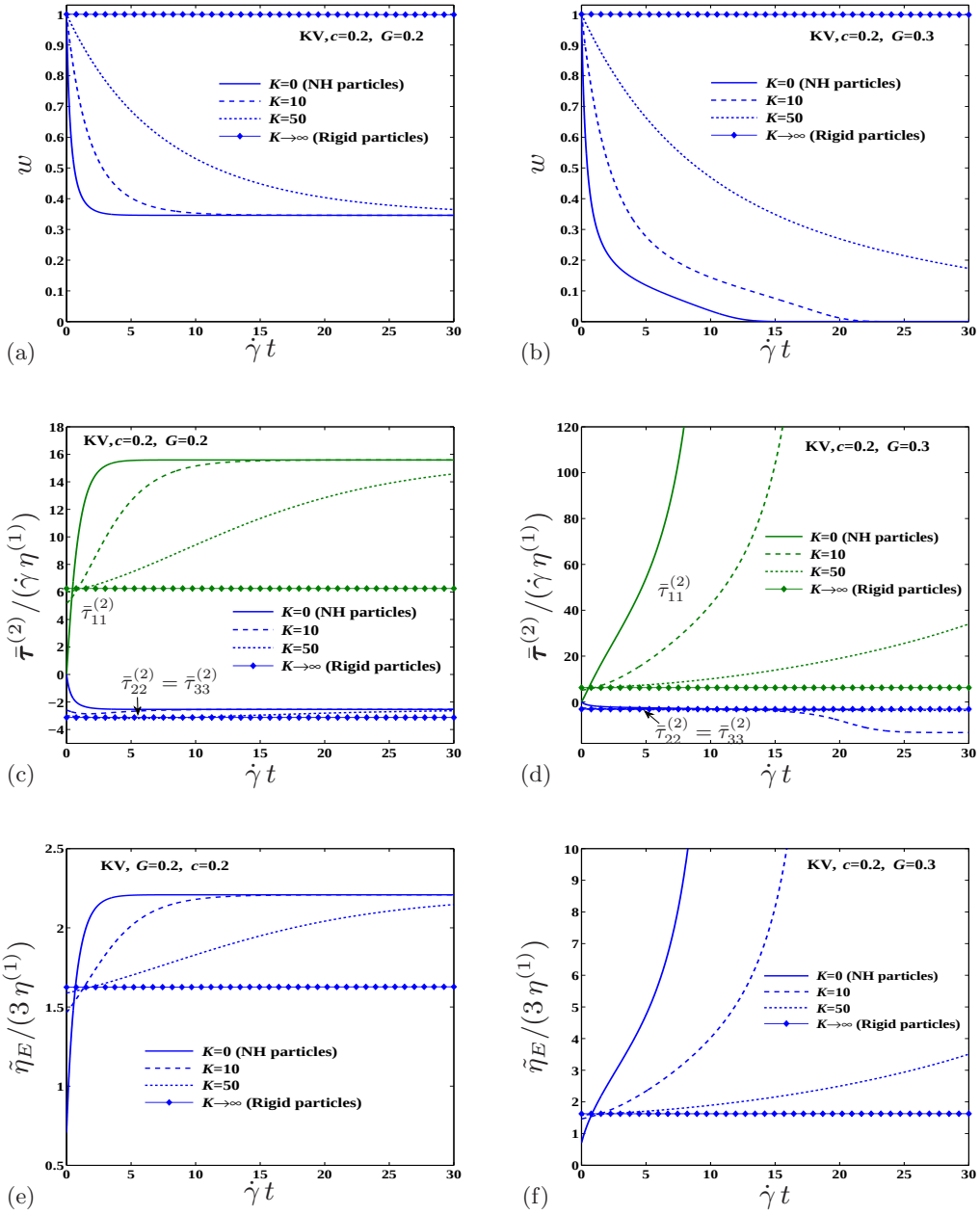

FIGURE 3. Results for the time-dependent response of suspensions of initially spherical Kelvin-Voigt particles (with NH elastic part) for $c = 0.2$ in an extensional flow. (a)-(b) Average aspect ratio of the particles. (c)-(d) Average extra stresses in the particles. (e)-(f) Relative viscosity of the suspension.

Kelvin-Voigt particles (with a NH elastic part) in an extensional flow. Results are shown for a fixed volume fraction ($c = 0.2$) and various values of the viscosity ratio K. Figures 3(a) and (b) show results for evolution of w calculated at $G = 0.2$ and $G = 0.3$, respectively. In the same way, figures 3(c) to (d) and (e) to (f) show results for the non-zero

components of $\bar{\boldsymbol{\tau}}^{(2)}$ and the viscosity $\tilde{\eta}_E$, respectively. It is recalled that the extreme limits $K = 0$ and $K \to \infty$ in these figures correspond to the cases of purely elastic and rigid particles, respectively. An important observation from figures 3(a), (c) and (e) is that the suspensions of KV particles reach the same steady state as in suspensions of NH particles, despite the evident differences in their respective time-dependent responses (this point will be explained in more detail shortly). In particular, we can see from figure 3(a) that the KV particles, before reaching the steady state, exhibit decreasing deformability as K increases. This produces smaller stresses in the particles (see figure 3 (c)), which results in smaller extensional viscosities in the suspension (see figure 3 (e)). Figures 3(b), (d) and (f) present corresponding results for a higher value of $G(= 0.3)$. For this larger value of G, the KV particles keep deforming as long as the applied stresses are large enough, and the suspension can not reach a steady state, similar to the case of purely elastic NH particles ($K = 0$) discussed in the context of figures 2(a), (c) and (e).

Next, we consider the steady-state response of the suspensions of initially spherical particles in the extensional flow (5.1). It follows from the symmetry of the problem that the shear components of the stress and strain rate are zero in the particle phase. Hence, for the case of KV particles, the steady-state stress in the particle phase is purely elastic, i.e. $\bar{\tau}^{(2)}_{ij} = (\bar{\tau}^{(2)}_e)_{ij}$ (this can be verified from relations (4.12) and (4.13) by noting that $\bar{D}_{ij} = 0$, $i \neq j$.) This implies that the SS values for the particle shape, stress and strain rate, in the suspensions of KV particles subjected to an extensional flow, are independent of the parameter K and, therefore, are equal to those corresponding to the elastic limit of the particles, characterized by $K = 0$. However, note that the case of $K \to \infty$ corresponds to rigid particles for which the particles do not deform. In this context, it is worthwhile to provide an expression for the steady-state value of the particle aspect ratio, denoted by w_s, in extensional flow. Thus, w_s is obtained as the acceptable root of the non-linear equation

$$4\,G\,\omega_{1s}^5 - (1-c)\,w_s^2\left[(w_s^2+2)\omega_{2s} - 6\,\omega_{1s}\right]\Delta_s = 0, \tag{5.6}$$

where the variables $\omega_{1s} = \sqrt{1-w_s^2}$ and $\omega_{2s} = 2\,\ln(\omega_{1s}+1) - 2\,\ln(w_s)$ are introduced for conciseness, and

$$\Delta_s = \begin{cases} J_m\,(1-w_s^2)/[(J_m+3)\,w_s^{(4/3)} - (2\,w_s^2+1)], & \text{for Gent particle,} \\ w_s^{-4/3}\,(1-w_s^2), & \text{for NH particle.} \end{cases} \tag{5.7}$$

The steady-state value of the effective viscosity (5.2) can also be obtained as

$$\tilde{\eta}_E = 3\,\eta^{(1)}\left(1 - c\,D_s + \frac{1}{3\,G}\,c\,\Delta_s\right), \tag{5.8}$$

where the variable D_s is given by

$$D_s = \frac{w_s^2\,(1-c)\left[(w_s^2+2)\omega_{2s} - 6\,\omega_{1s}\right]\Delta_s - 4\,G\,\omega_{1s}^5}{G\,\{3\,(1-c)\,w_s^2\,(w_s^2+2)\,\omega_{2s} - 2\,\omega_{1s}\,[2\,\omega_{1s}^4 + 9\,(1-c)\,w_s^2]\}}, \tag{5.9}$$

with w_s being the steady-state aspect ratio.

Figure 4 shows estimates for the SS value of the (extensional) effective viscosity for suspensions of (initially spherical) elastic particles. Figures 4(a) and (b) show plots as a function of G for neo-Hookean and Gent particles, respectively, while figures 4(c) and (d) show plots as a function of the volume fraction for neo-Hookean and Gent particles, respectively. We observe from figures 4(a), (b) and (c) that $\tilde{\eta}_E$ grows monotonically as G increases, indicating a shear-thickening effect in suspensions of NH and Gent particles. This growth is stronger at higher values of the particle volume fraction. Also, for the

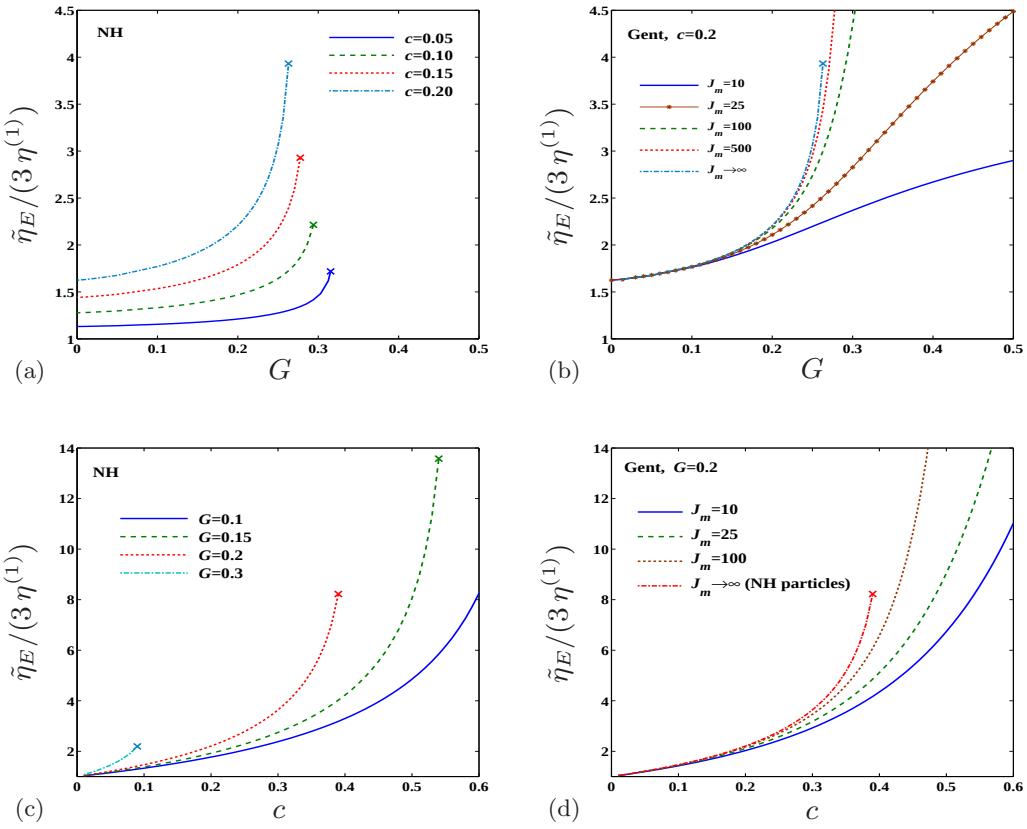

FIGURE 4. Results for the steady-state relative viscosities of suspensions of initially spherical, neo-Hookean and Gent particles in extensional flow.

case of NH particles, there is a critical value for G (marked with $\times$) beyond which the response of the suspension can not reach a steady state (refer to figure 2(e), and for which the time-dependent effective viscosity of the suspension tends to infinity.) However, as shown in figures 4(b) and (d), this unrealistic feature disappears for suspensions of Gent particles with a finite J_m in which case the time-dependent response reaches a steady state with a finite value for $\tilde{\eta}^E$. As discussed in the context of figure 2, this is because the Gent model provides a more realistic constitutive description of the elastomeric particles by capturing the experimentally observed, finite extensibility of such materials.

5.2. *Suspensions of initially spherical particles in a shear flow*

Next, we consider suspensions of initially spherical particles in a simple shear flow, characterized by

$$\bar{\mathbf{L}} = \dot{\gamma}\,\mathbf{E}_1 \otimes \mathbf{E}_2, \quad \bar{\mathbf{D}} = \frac{1}{2}\dot{\gamma}\,(\mathbf{E}_1 \otimes \mathbf{E}_2 + \mathbf{E}_2 \otimes \mathbf{E}_1), \quad \bar{\mathbf{W}} = \frac{1}{2}\dot{\gamma}\,(\mathbf{E}_1 \otimes \mathbf{E}_2 - \mathbf{E}_2 \otimes \mathbf{E}_1), \tag{5.10}$$

where the $\{\mathbf{E}_i\}$ refer to the fixed laboratory coordinates, and $\dot{\gamma} > 0$ is the shear strain rate. In this case, the initially spherical particles deform into ellipsoids of general shape characterized by the two aspect ratios w_1 and w_2, which in turn rotate remaining in the $\mathbf{E}_1 - \mathbf{E}_2$ plane in such a way that their current orientation may be described in terms of a single angle θ (measured positive in the counterclockwise direction from the $\mathbf{E}_1$ direction).

Then, the evolution equations (3.24) to (3.29) can be shown to specialize to equations (C 1) in Appendix C. This system of equations, together with relations (3.18) and (3.19), can be integrated numerically for the time-dependent solution. For completeness, the components of the shape tensors $\mathbb{P}$ and $\mathbb{R}$, required for this integration, are provided in Appendix D. Finally, given the current values of the elastic stresses $\bar{\boldsymbol{\tau}}_e^{(2)}$, aspect ratios w_1 and w_2 and orientation θ of the particles, the macroscopic stress $\bar{\boldsymbol{\sigma}}$ can be derived by means of expression (3.22), together with (3.18).

To conveniently describe the macroscopic response of the suspension in shear flow, we introduce the effective *shear viscosity*, as well as the first and second *normal stress differences* of the suspensions, defined by

$$\tilde{\eta}_S = \frac{1}{2\,\bar{D}_{12}}\bar{\sigma}_{12} = \frac{1}{\dot{\gamma}}\,\bar{\sigma}_{12}, \tag{5.11}$$

and

$$\Pi_1 = \bar{\sigma}_{11} - \bar{\sigma}_{22}, \qquad \Pi_2 = \bar{\sigma}_{22} - \bar{\sigma}_{33}, \tag{5.12}$$

respectively, where the components are relative to the fixed laboratory axes. Also, the corresponding *intrinsic viscosity* of the suspension is defined by

$$\tilde{\eta}'_S = \frac{1}{c}\left(\tilde{\eta}_S/\eta^{(1)} - 1\right), \tag{5.13}$$

and similarly for the intrinsic normal stress differences Π'_1 and Π'_2.

As was the case for extensional flow, we make use of the initial condition $\bar{\boldsymbol{\tau}}_e^{(2)}\Big|_{t=0} = \mathbf{0}$ to obtain the initial viscosity of the suspension. As already mentioned, at $t = 0$, the suspensions of KV particles behave like suspensions of spherical drops with viscosity ratio K. The initial relative viscosity $(\tilde{\eta}_S/\eta^{(1)})$ for this suspension is then given by

$$\left.\frac{\tilde{\eta}_S}{\eta^{(1)}}\right|_{t=0} = \frac{(3c+2)\,K + 3\,(1-c)}{2\,(1-c)\,K + 2\,c + 3}. \tag{5.14}$$

For the case of elastic particles ($K = 0$), the above relation reduces to

$$\left.\frac{\tilde{\eta}_S}{\eta^{(1)}}\right|_{t=0} = \frac{1-c}{1+2\,c/3}. \tag{5.15}$$

Before proceeding with the detailed examples, it is emphasized that the components of the stress and strain rate tensors in the particle phase are shown below relative to the instantaneous principal axes of the particle.

Figure 5 shows estimates for the time-dependent response of dilute and non-dilute suspensions of initially spherical NH particles in a shear flow. The results are given for $G = 0.2$ and various values of particle volume fraction. Figure 5 (a) and (b) depict the evolutions for the aspect ratios w_1 and w_2 and the particle orientation angle θ, respectively. It is helpful to recall that w_1 and w_2 correspond to the aspect ratios of the particle in the plane of the flow and in the plane perpendicular to the short in-plane axis of the particles, respectively. The evolutions of w_1, w_2 and θ in figures 5 (a) and (b) indicate that the particles in suspensions with a higher volume fraction become more elongated and their major axis becomes more aligned with the shear direction, before reaching a steady state. We emphasize that while the particle shape and orientation do not change in the steady state, material points in the particle undergo a periodic *tank-treading* motion. This motion has been frequently reported in suspensions of red blood cells (see, e.g., Keller & Skalak (1982)) and capsules (Clausen & Aidun 2010; Clausen *et al.* 2011), in which the enclosing membrane continues to rotate around the interior

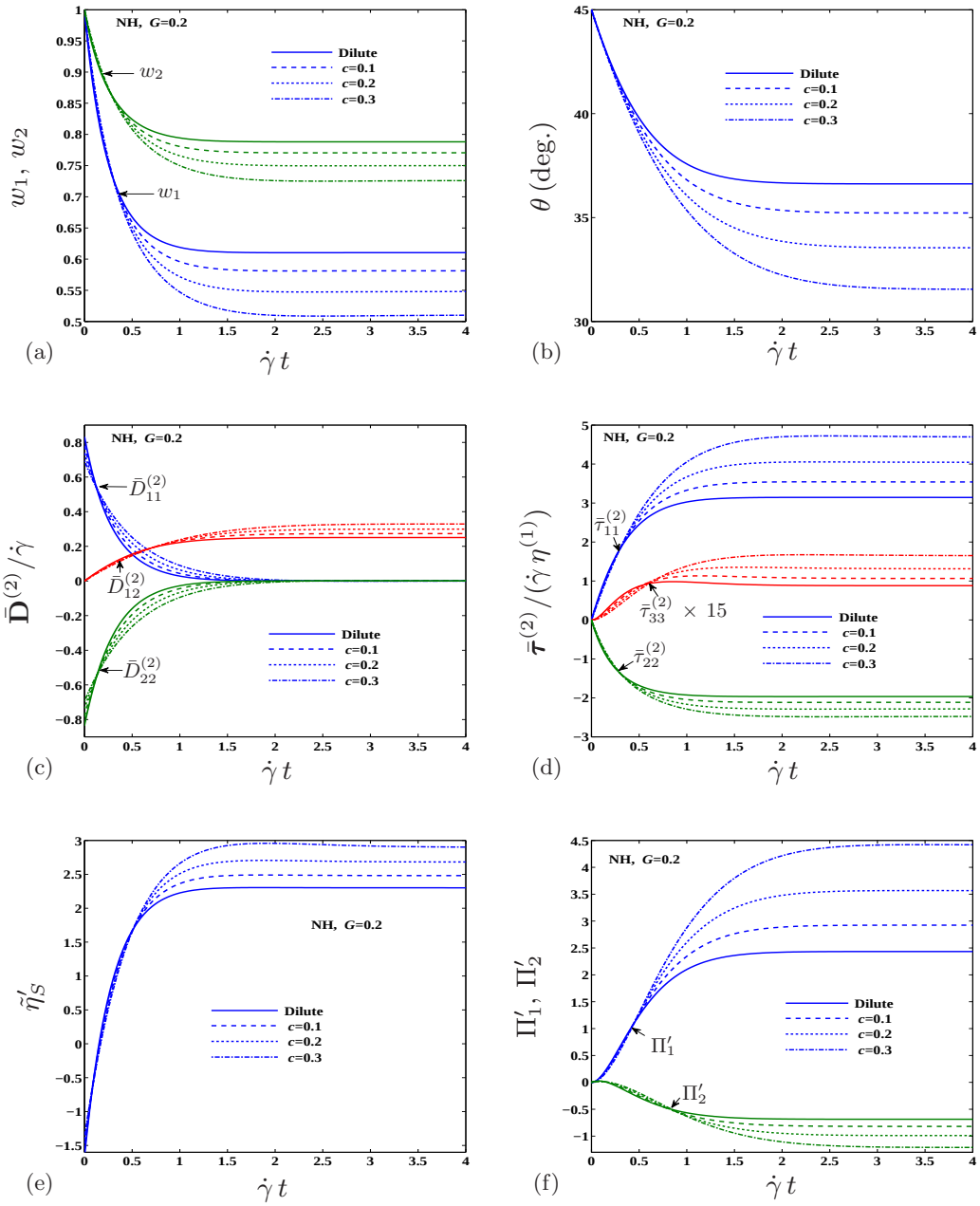

FIGURE 5. Results for the time-dependent response of suspensions of initially spherical neo-Hookean particles with $G = 0.2$ and various values of c in a shear flow. (a) In-plane (w_1) and out-of-plane (w_2) average aspect ratios of the particles. (b) Average (in-plane) inclination angle of the particles. (c) Average strain-rates in the particles (relative to the principal axes of the particle). (d) Average extra stresses in the particles (relative to the principal axes of the particle). (e) Intrinsic viscosity of the suspension. (f) Corresponding "intrinsic" values of the normal stress differences in the suspension (relative to the laboratory coordinates).

fluid in a tank-treading motion. As can be seen from figures 5 (c) and (d), the normal components of the strain rate (relative to the instantaneous axes of the particle) decay to zero with the deformation, while the shear component of the strain rate and normal components of the extra elastic stress in the particles build up from zero until reaching their steady-state values. Also, we observe from figure 5(d) that the normal components of the average stress in the particles exhibit a progressive increase (in magnitude) as the volume fraction of the particles increases, which, correspondingly, leads to a higher intrinsic viscosity and normal stress differences, as can be seen in figures 5(e) and (f).

Figures 6(a) to (c) depict estimates for the time-dependent behavior of the particle shape and orientation in suspensions of NH particles with $c = 0.2$ in shear flows with varying values of G. The results suggest that the NH particles exhibit larger stretches, which increase monotonically with increasing values of G. For the largest value of G (i.e., $G = 1.5$ for this figure), we have also included the corresponding results for Gent particles with $J_m = 5$. For this case, we observe a significant reduction in the level of deformation resulting from the inextensibility constraint. On the other hand, figures 6(d) and (f) show the corresponding time-dependent results for the effective viscosity and normal stress differences. We observe from figure 6(d) that the initial value of the effective shear viscosity is independent of the value of G and is approximately equal to 0.7 (this matches the value calculated from (5.15) for $c = 0.2$.) We further observe that the time-dependent behavior of the effective viscosity and the first normal stress shows a more pronounced "overshoot" with increasing values of G. As explained by Gao *et al.* (2011), the overshoot and the subsequent decay observed in these figures are due to the fact that the particles rotation continues even after the particles have stopped elongating in the plane of shear (see figures 6(a) and (c).) Consistently, we notice from figures 6(a) and (c) that the time interval between the arrest of the particles elongations in the plane of shear and the corresponding arrest of the particles rotations becomes progressively larger as G increases. Finally, we observe from figure 6(d) that the SS value of the effective viscosity drops as the value of G increases which suggests a *shear-thinning* effect.

Figure 7 shows estimates for the time-dependent rheological behavior of suspensions of KV particles in shear flow. In particular, we investigate the influence of the viscosity of the particles, characterized by the parameter $K = \eta^{(2)}/\eta^{(1)}$, on the time-dependent behavior, calculated at fixed values $G = 0.2$ and $c = 0.2$. We recall that the extreme cases $K = 0$ and $K \to \infty$ correspond to suspension of purely elastic and rigid particles, respectively. We observe from figures 7(a) and (b) that, for low values of K, the motion of the particles follows the same general trends as those of the purely elastic particles. However, for higher values of K, the particles undergo a *damped oscillatory* motion of decreasing amplitude before reaching the steady state. This motion is similar to that observed for capsules under similar flow conditions, as reported by Clausen *et al.* (2011). In the limit of rigid particles ($K \to \infty$), the rotation of particles is entirely given by the rigid body rotation of the imposed shear flow, i.e. $\theta = \pi/4 - \dot{\gamma}\, t/2$. Figure 7(c) shows the components of the extra stress tensor in the particle ($\bar{\boldsymbol{\tau}}^{(2)}$) relative to the principal axes of particles. It is interesting to note that, for the case of KV particles ($K \neq 0$), the shear component $\bar{\tau}_{12}^{(2)}$ has a non-zero value, which has no contribution from the elastic part of the stress, i.e. $\bar{\tau}_{12}^{(2)} = (\bar{\tau}_v^{(2)})_{12} = 2\,\eta^{(2)}\,\bar{D}_{12}^{(2)}$. Next, figures 7(d), (e), and (f) show the corresponding effective viscosity, first and second normal stress differences of the suspensions, respectively. As expected, it can be seen from figure 7(d) that the values of the effective viscosity at $t = 0$ match the corresponding values calculated from relation (5.14). Also, we observe from figure 7(f) that, at higher values of K, the second normal

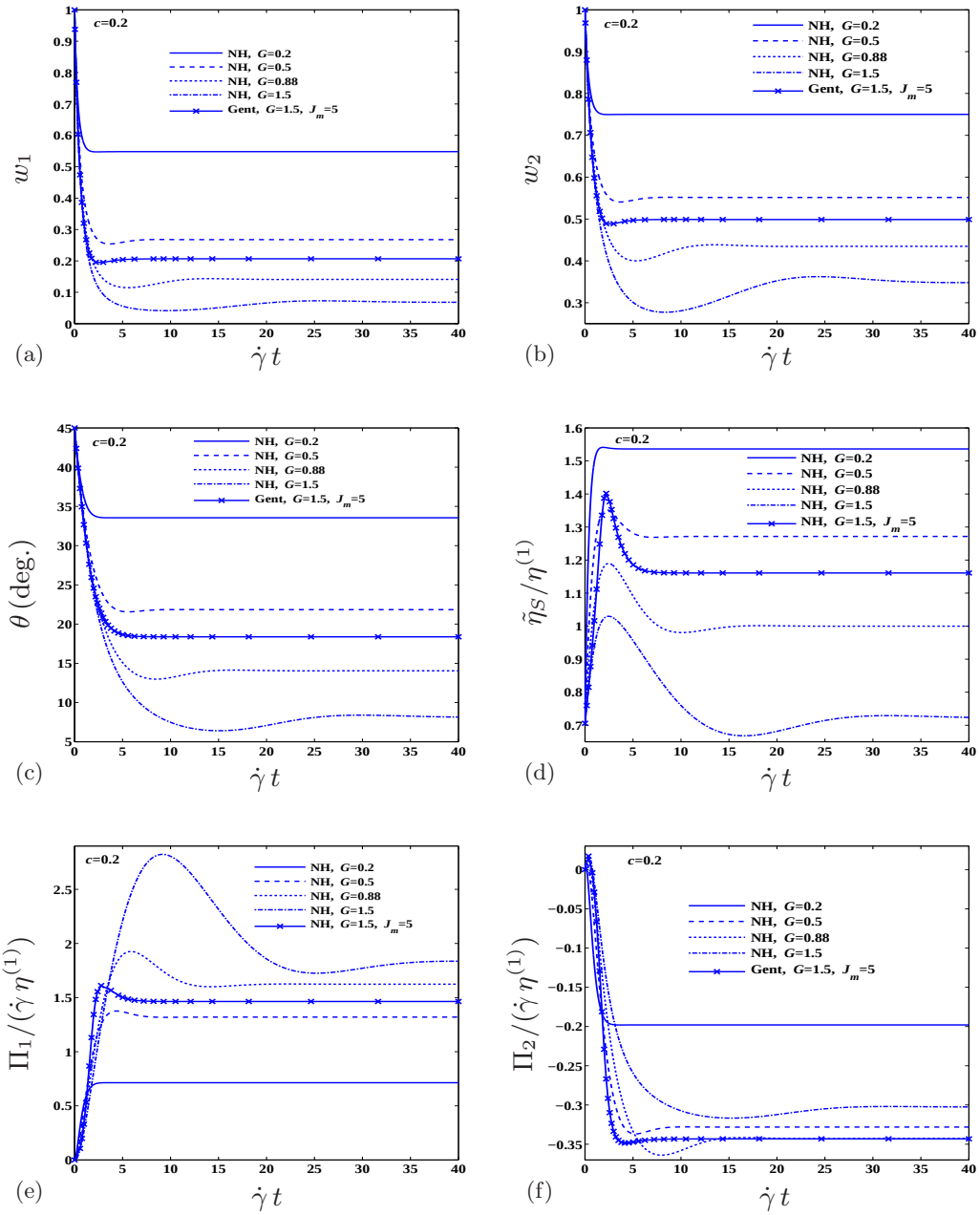

FIGURE 6. Results for the time-dependent response of suspensions of initially spherical neo-Hookean and Gent particles with $c = 0.2$ and various values of the dimensionless parameter G in a shear flow. Higher values of G correspond to softer particles, or to larger shear-strain rates. (a) In-plane and (b) out-of-plane average aspect ratios of the particles. (c) Average (in-plane) inclination angle of the particles. (d) Relative viscosity of the suspension. (e) and (f) Normal stress differences in the suspension (relative to the laboratory coordinates).

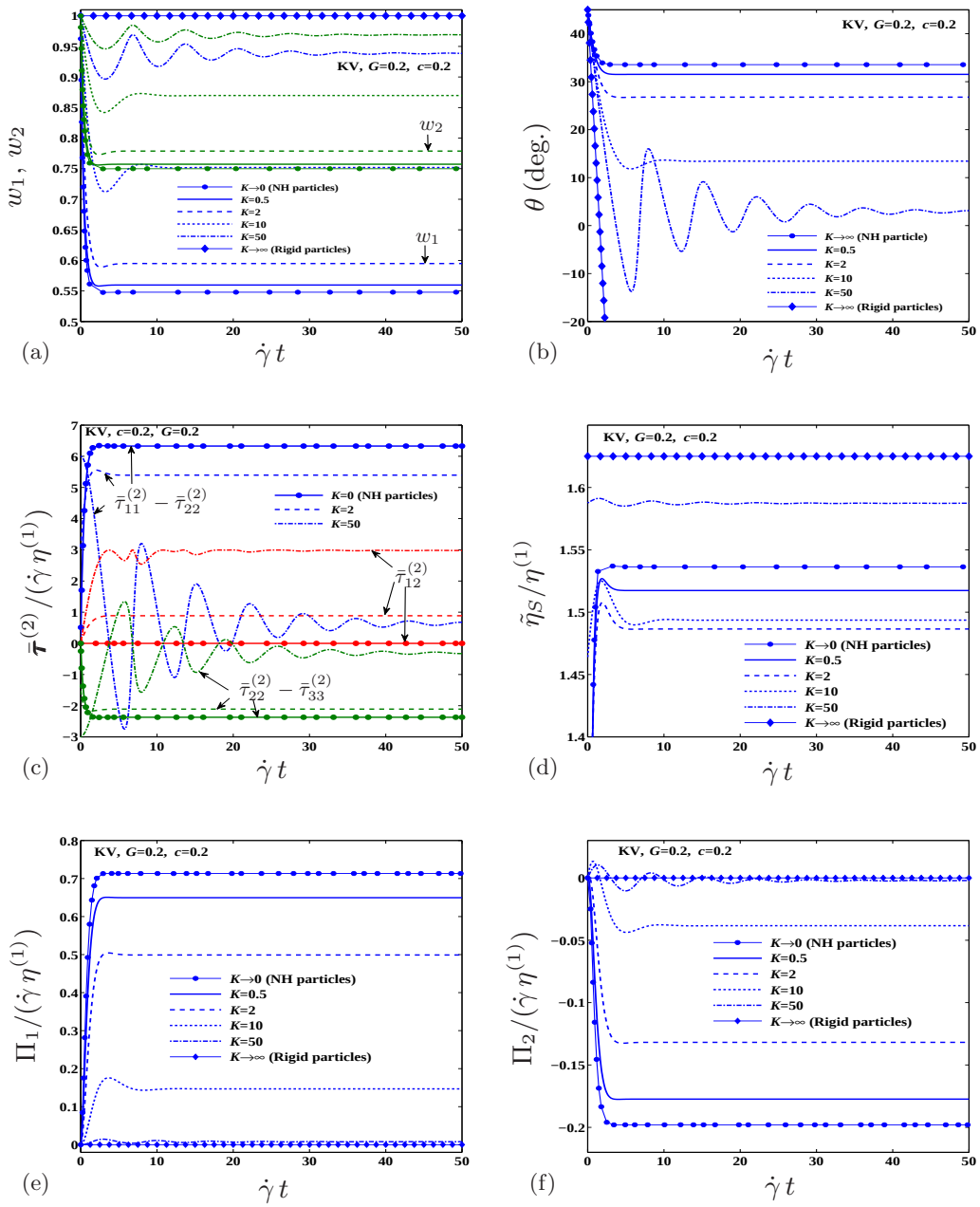

FIGURE 7. Results for the time-dependent response of suspensions of initially spherical Kelvin-Voigt particles (with NH elastic part) with $G = 0.2$ and various values of K in a shear flow. (a) In-plane (w_1) and out-of-plane (w_2) average aspect ratios of the particles. (b) Average inclination angle of the particles. (c) Average extra stresses in the particles (relative to the principal axes of the particle). (d) Relative viscosity of the suspension. (e) and (f) Normal stress differences in the suspension (relative to the laboratory coordinates).

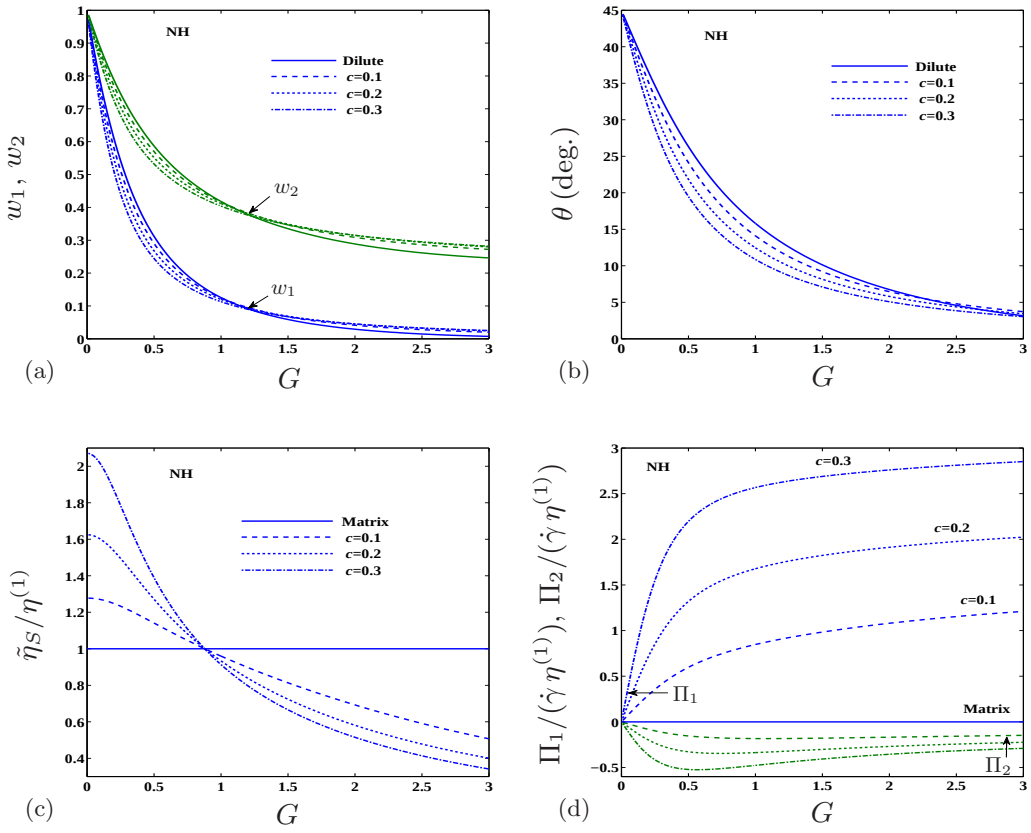

FIGURE 8. Results for the steady-state response of suspensions of initially spherical neo-Hookean particles for various values of c in a shear flow. (a) In-plane and out-of-plane average aspect ratios of the particles. (b) Average inclination angle of the particles. (c) Relative viscosity of the suspension. (d) Normal stress differences in the suspension (relative to the laboratory coordinates).

stress difference has an initial overshoot with positive values, similar to the results for the case of suspensions of concentrated capsules, as reported by Clausen *et al.* (2011).

Next, we investigate the steady-state response of the suspensions of neo-Hookean particles under the shear flow conditions (5.10). Figures 8(a) and (b) show estimates for SS values of the aspect ratios and orientation of the particles, respectively, as a function of G, for several values of the particle volume fraction. These figures indicate that, as G increases, the NH particles reach larger elongations, as well as closer alignments with the shear direction at the steady state. This behavior of the particles is seen to be weakly affected by the value of c. Next, figure 8(c) and (d) show the corresponding estimates for the effective viscosity and normal stresses, respectively. We observe from figure 8(c) that the effective viscosity $\tilde{\eta}_S$ decreases as G increases, thus showing a shear-thinning response. Moreover, when $G \to 0$, which corresponds to suspensions of rigid spherical particles, we recover the Saito (1950) formula (also the Hashin-Shtrikman lower bound), as given by

$$\left.\frac{\tilde{\eta}_S}{\eta^{(1)}}\right|_{G\to 0} = \frac{1+3\,c/2}{1-c}. \tag{5.16}$$

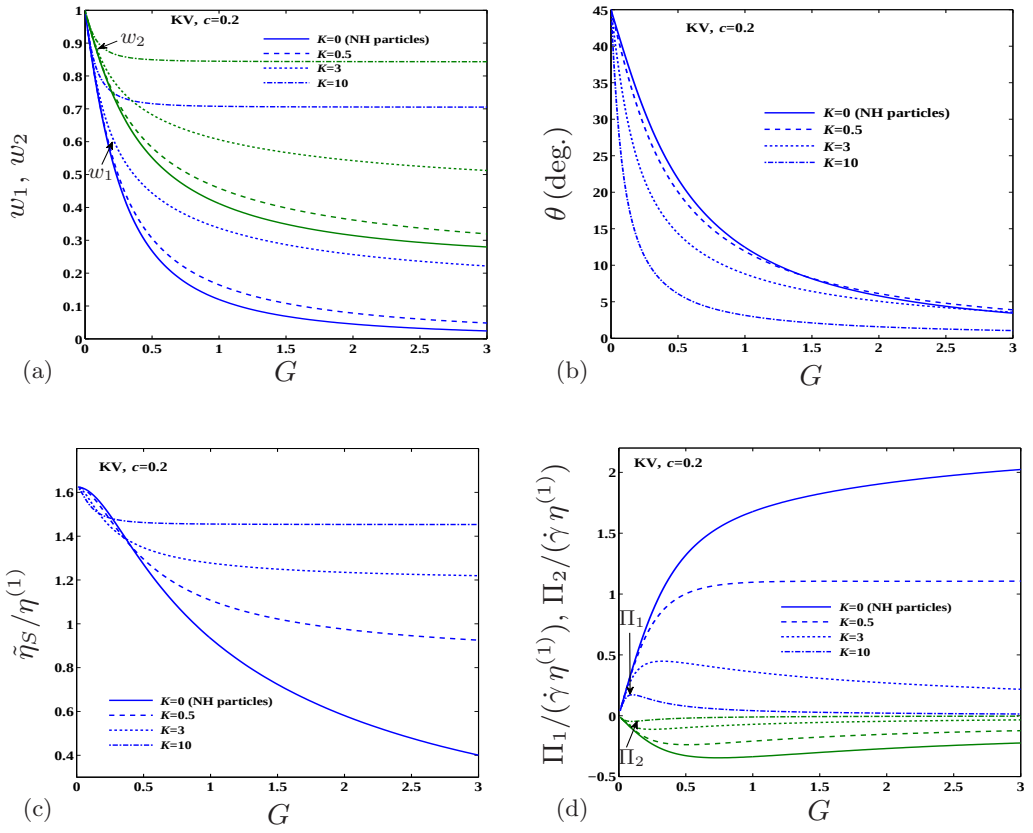

FIGURE 9. Results for the steady-state response of suspensions of initially spherical Kelvin-Voigt particles (with NH elastic behavior) for various values of K in a shear flow. (a) In-plane and out-of-plane average aspect ratios of the particles. (b) Average inclination angle of the particles. (c) Relative viscosity of the suspension. (d) Normal stress differences in the suspension (relative to the laboratory coordinates).

Another interesting observation from figure 8(c) is that, at approximately $G = 0.88$, the relative viscosity becomes unity. This implies that, at this value of G, the suspended elastic particles do not change the effective viscosity of the host liquid. Particles having this property have been found in other physical phenomena (Milton 2002) and are known in the literature as "neutral" particles. We observe from figure 8(c) that the value of G at which the NH particles become neutral, G_N say, has a weak dependence on the volume fraction of the particles (G_N is slightly smaller than 0.88 for $c > 0.3$.) For $G > G_N$, the effective viscosity of the suspension is actually less than unity, similar to the case of suspensions of viscous droplets in a more viscous liquid.

Figure 9 presents estimates for the SS behavior of the particles, as well as for the associated macroscopic rheological properties, of suspensions of KV particles (with NH elastic behavior) subjected to shear flow conditions. Figure 8(a) and (b) show results for the aspect ratios and orientations of the particles, respectively, at several values of K, for a fixed value of $c = 0.2$. As expected, we observe from these figures that, for a fixed value of G, but for increasing values of K, the particles behave more like stiff particles by deforming less and rotating more, recovering the case of rigid particles in the limit of

$K \to \infty$. Figures 9(c) and (d) show results for the corresponding effective viscosity and normal stress differences, respectively. We observe from these figures that the viscosity of the particles (controlled by the parameter K) has a more significant effect on the steady-state behavior of the suspension at higher values of G. In addition, we observe from figure 9(a) that the value of G_N, at which the particles become neutral ($\tilde{\eta}_S = \eta^{(1)}$), increases with K up to a certain value of K, beyond which the particles may never become neutral.

Next, in figure 10, we investigate the influence of the particle volume fractions on the SS values of the effective viscosity and normal stress differences of suspensions with different types of particles. Thus, figures 10(a) to (b), (c) to (d), and (e) to (f) show plots as functions of c for neo-Hookean, Gent and Kelvin-Voigt (with NH elastic behavior) particles, respectively. Consistent with earlier comments in the context of figure 8, we observe from figure 10(a) that, for suspensions of NH particles with $G < 0.88$, the relative viscosity ($\tilde{\eta}_S/\eta^{(1)}$) is greater than unity and increases with increasing particle concentration c, while for for suspensions with $G > 0.88$, the relative viscosity is less than one and decreases with increasing values of c. For $G \approx 0.88$, the relative viscosity is close to one and is fairly insensitive to the particle concentration. On the other hand, we see from figure 10(c) that, even at a high value of $G(= 2)$, the relative viscosity of suspensions of Gent particles with a small enough value of J_m, can still be greater than unity and exhibits monotonic growth in c. Furthermore, we note from figure 10(e) that the viscosity of KV particles with $G = 0.2$ has a weak effect on the relative viscosity of the suspension up to moderate levels of concentration ($c < 0.3$). In addition, it is observed from figures 10 (b), (d) and (f) that the magnitude of the normal stresses always increases with the particle concentration c, but is fairly insensitive to the values of G and J_m, although a little more sensitive to the viscosity ratio K.

Finally, comparisons are shown in figure 11 of the model's predictions with numerical simulation results for suspensions of capsules, as well as with experimental data for suspensions of red blood cells (RBCs) under shear flow conditions. While our model has been developed to describe the effective response of suspensions of "homogeneous" viscoelastic particles, we have not been able to find a sufficiently complete set of experimental results (including the constitutive properties of the particles) to make the appropriate comparisons. In particular for this reason, but also because it is interesting to explore possible connections with "inhomogeneous" particles, we will make here "qualitative" comparisons with experimental results for suspensions of capsules and cells, by making appropriate choices for the properties of the KV particles, Thus, figures 11(a) to (d) show comparisons between our model results for dilute suspensions of KV particles and the corresponding simulation results of Ramanujan & Pozrikidis (1998) for dilute suspensions of spherical capsules in a shear flow. The initially spherical capsules are composed of a fluid-filled interior (with radius a) enclosed by a NH elastic membrane (with shear modulus μ_m), where the viscosity of the internal fluid is equal to that of the external suspending fluid. The dimensionless parameter $G_m = \eta^{(1)}\dot{\gamma}\, a/\mu_m$ for the capsules is the counterpart of the parameter G for the KV particles. Then, a plausible choice for the properties of the KV particles (with a NH elastic response) in our model would be $G = G_m$ and $K = 1$. Figures 11(a) and (b) show the comparisons for the time-dependent behavior of the Taylor deformation parameter $D = (1 - w_1)/(1 + w_1)$ and the particle orientation, respectively, while figures 11(c) and (d) show the comparisons for the time-dependent behavior of the excess (or intrinsic) viscosity and the normal stress differences, respectively. Surprisingly, the comparisons are actually quite good, at least for these dilute concentrations. Although the KV particles correspond to an extremely simple microstructural element consisting of a linear dashpot connected in parallel with an NH spring, the model seems to be able to capture—at least in qualitative terms—the

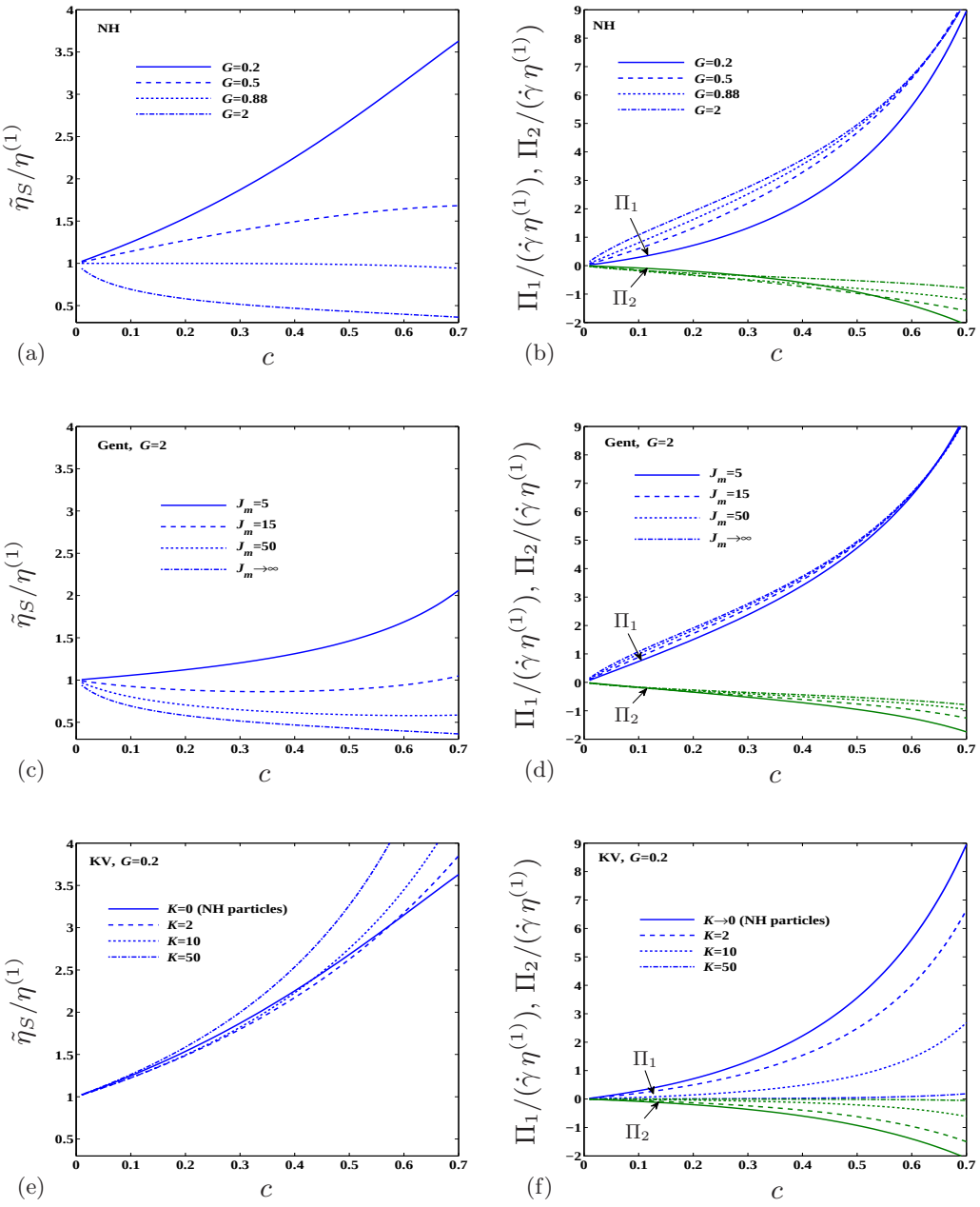

FIGURE 10. Results for the steady-state relative viscosity and normal stress differences of suspensions of initially spherical (a)-(b) neo-Hookean, (c)-(d) Gent and (e)-(f) Kelvin-Voigt particles (with NH elastic part) in a shear flow.

macroscopic features of the suspensions of capsules, which correspond to a much more complex microstructural element consisting of a linearly viscous drop enclosed by a NH membrane.

Next, in figure 11(e), comparisons are given between results for the steady-state re-

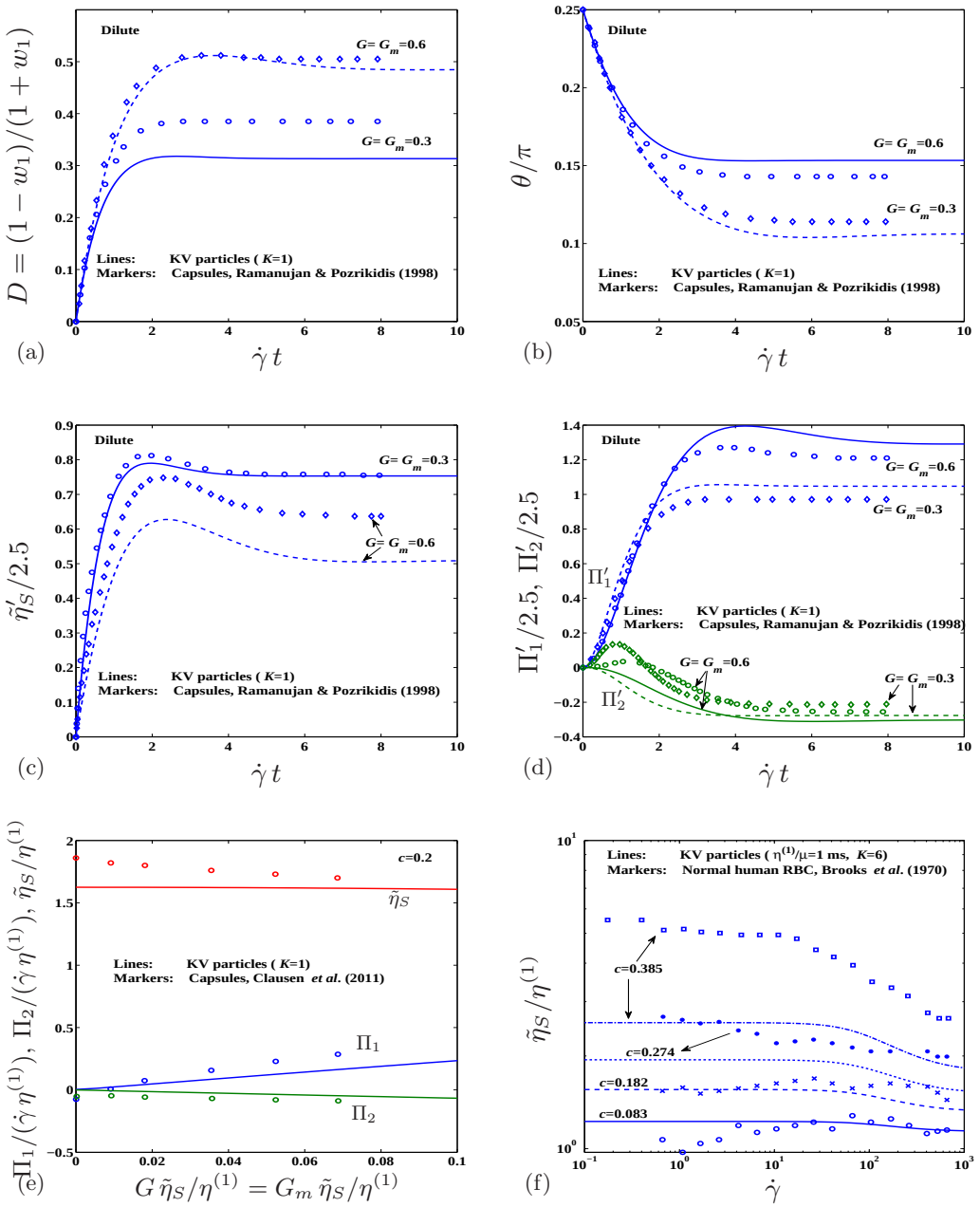

FIGURE 11. Comparisons of the predictions of our model with numerical simulation results for suspensions of initially spherical capsules, as well as with experimental data for suspensions of RBCs under shear flow conditions. Comparisons of the time-dependent (a) Taylor deformation parameter, (b) average inclination angle, (c) intrinsic viscosity, and (d) intrinsic normal stress differences for dilute suspensions of KV particles with the simulation results of Ramanujan & Pozrikidis (1998) for the corresponding response of dilute suspensions of capsules. (e) Comparisons of the SS response of suspensions of KV particles with the simulation results of Clausen *et al.* (2011) for the SS behavior of non-dilute suspensions of capsules. (f) Comparisons of the SS behavior of suspensions of KV particles with the experimental data of Brooks *et al.* (1970) for the effective viscosity of suspensions of normal human RBCs, as a function of the shear rate $\dot{\gamma}$, for different values of the RBC volume fraction.

sponse of non-dilute suspensions of KV particles and the simulation results of Clausen *et al.* (2011) for suspensions of NH capsules in a shear flow. Results are shown for the effective viscosity and the normal stress differences for $c = 0.2$, as functions of $G\,\tilde{\eta}_S/\eta^{(1)}$. We observe from this figure that our model results are still in quite good agreement with the simulation results for the capsules, although the agreement becomes less good as the particle volume fraction increases (results not shown). In addition, it should be recalled that the model developed in this work is not expected to provide accurate predictions for rigid particles, corresponding to a zero value for G in the figure, as a consequence of the fact that the shape of (the angular dependence of) the two-point correlation function has been assumed (for simplicity) to be identical to that of the particles. Since for rigid particles, the particle shape cannot change, this would mean that the two-point correlations function remains isotropic, which is not expected to be the case for the non-Brownian suspensions considered in this work. As already stated, for deformable particles ($G > 0$), the changes in shape and orientation of the particles are expected to dominate the higher-order effect (in c) of the corresponding changes in the particle distribution, and the model is expected to be more accurate in these cases.

Lastly, figure 11(f) shows comparisons between the predictions of our model and the experimental data of Brooks *et al.* (1970) for the effective viscosity of suspensions of normal human RBCs in a shear flow, as a function of the shear rate $\dot{\gamma}$, for different values of the RBC volume fraction. The RBCs consist of a thin elastic membrane with shear modulus $\sim 4 \times 10^{-6}$N/m and the average radius $4\,\mu$m, filled with a nearly Newtonian fluid with viscosity $6 - 7$ mPa.s. Also, the suspending fluid is a protein-free saline with the viscosity $1 - 1.2$ mPa.s. Similar to the case of capsules, we can use our model to estimate the rheological properties of suspensions of RBCs by appropriately choosing K and $\eta^{(1)}/\mu$. Consistent with the above-mentioned RBCs properties, we choose $\eta^{(1)}/\mu = 1\,ms$ and $K = 6$. The predictions of our model in figure 11(f) show quite good agreement with the experimental data for small volume fractions ($c < 20\%$). For higher volume fractions, our results can still capture the shear-thinning behavior exhibited by the suspensions of RBCs at the higher shear rates. However, the magnitude of the effect is under-predicted by our model, which is probably due to the fact that the variational estimates of the PCW-type tend to under-predict the strong interaction effects that develop among the particles at the higher particle concentrations ($c > 20\%$) for mono-disperse systems.

6. Conclusions

In this paper, we have developed a homogenization model characterizing the finite-strain, time-dependent response of non-dilute suspensions of micro-scaled, deformable particles in a Newtonian fluid under Stokes flow conditions. Although more general initial shapes (e.g., ellipsoidal) and viscoelastic constitutive models (e.g., Jeffreys) could be used for the particles, we have considered here suspensions of initially spherical particles whose constitutive response is characterized by Kelvin-Voigt (KV) behavior incorporating finite extensibility of the particles in the regime of arbitrarily large deformations. Our model is based on the homogenization theory of Ponte Castañeda & Willis (1995) for linear-elastic composite materials with particulate microstructures. Extended in the manner initially suggested by Kailasam & Ponte Castañeda (1998) to account for viscous behavior and finite strains, this technique has been used here to generate estimates for the averages of the strain rate and vorticity tensors in the particle phase, as given by equations (3.18) and (3.19), respectively. Such estimates, together with evolution equations for the elastic stress in the particles, as given by (3.27), and for the average particle shape and orientation, as given by (3.24) and (3.25), respectively, can then be used to obtain estimates

for the macroscopic stress of the suspension by means of equation (3.22). The resulting constitutive model provides a complete description for the time-dependent, macroscopic, rheological response of the *non-dilute* suspensions of *viscoelastic* particles under macroscopically uniform flows, thus generalizing earlier work by Gao *et al.* (2011) for *dilute* suspensions of neo-Hookean (NH) *elastic* particles. However, it should be emphasized that, because of restrictions associated with the underlying homogenization technique (Ponte Castañeda & Willis 1995), the model is more appropriate for poly-disperse suspensions, although it could also be used for mono-disperse suspensions, provided that attention is restricted to small to moderate particle volume fractions. In addition, it should also be recalled that the model has made use of a rather simplistic (slave-type) evolution law for the two-point correlation function of the particle centers, and should not be used for suspensions of (nearly) rigid particles. Improvements to account for independent changes in the particle distribution correlation function are certainly possible, but they would probably make most sense in the context of more sophisticated homogenization methods incorporating higher-order statistics (Milton 2002).

We have also used the model developed in this work to explore the rather rich and complex rheological behavior of the deformable-particle suspensions by focusing on two types of flows: *extensional*, and *simple shear* flows. These examples provide a broad picture of the influence of the flow conditions, constitutive behaviors of the particles, and the particle volume fractions on the dynamics of the suspended particles, as well as on the macroscopic rheology of the suspension. For the case of extensional flows, we found that there is a critical value of the dimensionless parameter $G = \eta^{(1)}\,\dot{\gamma}/\mu$, beyond which suspensions of KV particles with NH elastic behavior cannot reach a steady state, and that this critical value of G decreases with increasing particle volume fraction. For dilute concentrations of the KV particles, this critical value agrees exactly with the corresponding results of Roscoe (1967). In addition, we showed that, when the value of G is subcritical and a steady state is reached, the viscosity of KV particles does not affect the rheological behavior of the suspension, although it does affect significantly the time-dependent response prior to reaching the steady state. On the other hand, for more realistic KV particles with Gent-type elastic behavior (exhibiting finite limits of extensibility characterized by the parameter J_m), the corresponding results indicate that steady-state (SS) solutions are available for the *full range* of values of G. In such cases, the corresponding SS values of the effective extensional viscosities exhibit shear-thickening and are lower for particles with a tighter extensibility constraint (lower values of J_m).

For simple shear flows, the viscoelastic properties of the initially spherical particles are found to have a significant effect on both the time-dependent and steady-state response of the suspension. For particles with a high viscosity ratio K, the particles exhibit *damped oscillatory* transient motions, before reaching a steady-state, tank-treading motion with fixed particles shapes and orientations. Similar motions have also been reported in the context of suspensions of initially spherical capsules by Clausen *et al.* (2011). On the other hand, the results of Gao *et al.* (2012) for dilute concentrations of purely elastic particles showed "trembling" (oscillatory) motions *only* for non-spherical initial shapes for the particles, indicating more complex behaviors for viscoelastic particles. Moreover, contrary to the SS results for extensional flows in which softer particles tend to increase the effective viscosity of the suspension, the corresponding SS results show that softer particles tend to reduce the effective viscosity in simple shear, and the suspension is found to exhibit an overall shear-thinning effect. However, it is interesting to note that, the shear-thickening/thinning effect is more pronounced for suspensions with higher particle volume fractions for both cases. Furthermore, in agreement with earlier results by Gao *et al.* (2011) for dilute concentrations, it has been found that the SS relative viscosity

of the suspension in shear can become unity at some critical value $G = G_N \approx 0.88$, beyond which it becomes less than one. This result suggests that it should be possible to design suspensions of "neutral" particles (Milton 2002), as well as suspensions with lower viscosity than that of the suspending fluid. Our results show that the value of G_N depends weakly on the volume fraction of the particles. However, for the case of Gent-type particles, the value of G_N is strongly dependent on the value of J_m, such that the smaller the J_m, the higher the G_N. It is also important to emphasize that, as the steady state is approached for simple shear flow conditions, the model predicts the development of significant normal stress differences, which are comparable in magnitude to the corresponding changes in the effective viscosity of the suspensions. These effects are a consequence of the development of microstructural anisotropy in the suspension, and have been neglected by earlier effective-medium treatments of the problem (see, for example, Snabre & Mills 1999; Pal 2003).

Finally, we made comparisons of the predictions of our model with simulation results for suspensions of capsules (composed of an interior fluid enclosed by a NH membrane), as well as with the experimental data for the suspensions of RBCs, in a shear flow. It was found that the predictions of the model (for appropriate choices for the properties of the KV particles) are in surprisingly good agreement with the simulation results for dilute suspensions of capsules. For non-dilute suspensions, the corresponding predictions start to deviate from the simulation results and experimental data at sufficiently large particle concentrations, but they are still in relatively good qualitative agreement with both simulation and experimental results. These comparisons suggest that simpler, *analytical* constitutive models for suspensions of viscoelastic particles (with uniform properties), such as the one developed in the present work, may be useful in describing at least some of the macroscopic rheological features of suspensions of more complex particles with non-uniform properties, possibly including capsules and vesicles. Such simplified constitutive models have the further advantage that they can be easily implemented numerically for use in standard finite element codes (Aravas & Ponte Castañeda 2004).

Acknowledgements

This material is based upon work supported by the National Science Foundation, which began under Grant No. CMMI-0969570 and was completed under Grant No. CMMI-1332965.

Appendix A. The Hashin-Shtrikman-Willis variational estimates

Hashin & Shtrikman (1963) introduced a variational technique to estimate the effective behavior of linear-elastic composites with statistically isotropic microstructures. This work was extended later by Willis (1977, 1981) for composites with more general anisotropic microstructures. For the particulate material systems of interest in this work, consisting of random distributions of ellipsoidal inclusions in a given matrix, more explicit estimates have been given by Ponte Castañeda & Willis (1995). Given the well-known analogy between the governing equations for a linear-elastic solid and a linearly viscous fluid, Kailasam *et al.* (1997) and Kailasam & Ponte Castañeda (1998) applied and generalized the PCW theory to estimate the instantaneous response of two-phase linearly and nonlinearly viscous composites subjected to simple flows, assuming that surface tension, buoyancy and dynamical effects could be neglected. In this appendix, we demonstrate how this earlier work for viscous composites can still be further generalized to provide

corresponding estimates for the class of suspensions of finitely deforming, viscoelastic particles considered in this work.

We begin by recalling expressions (3.8) and (3.10) defining the local dissipation potential W of the suspension. We then introduce a homogeneous "comparison" Newtonian fluid with viscosity η^0, whose dissipation potential is given by

$$W^0(\mathbf{D}) = \eta^0 \mathbf{D}\cdot\mathbf{D}, \quad \mathrm{tr}(\mathbf{D}) = \mathbf{0}. \tag{A 1}$$

Suppose for now that $\eta^0 \geq \eta^{(1)}, \eta^{(2)}$, so that $W - W^0$ is a concave function of $\mathbf{D}$. Then, following Talbot & Willis (1985), the Legendre-Fenchel transform of this difference potential can be defined as

$$\left(W - W^0\right)^*(\mathbf{x}, \boldsymbol{\Xi}) = \inf_{\mathbf{D}} \left\{\boldsymbol{\Xi}\cdot\mathbf{D} - [W(\mathbf{x},\mathbf{D}) - W^0(\mathbf{D})]\right\}. \tag{A 2}$$

Note that the stationary condition associated with this relation is

$$\boldsymbol{\Xi} = \boldsymbol{\tau} - 2\,\eta^0 \mathbf{D}, \tag{A 3}$$

where we have used the fact that $\boldsymbol{\tau} = \partial W/\partial \mathbf{D}$. As a consequence, the quantity $\boldsymbol{\Xi}$ is known as the "polarization" stress tensor relative to the comparison fluid. Noting that $\left(W - W^0\right)^*$ is concave, we deduce from (A 2), by Legendre duality, that

$$W(\mathbf{x},\mathbf{D}) = \inf_{\boldsymbol{\Xi}} \left\{W^0(\mathbf{D}) + \boldsymbol{\Xi}\cdot\mathbf{D} - \left(W - W^0\right)^*(\mathbf{x},\boldsymbol{\Xi})\right\}. \tag{A 4}$$

Substituting (A 4) into expression (3.16), and interchanging the order of infima over $\mathbf{D}$ and $\boldsymbol{\Xi}$, we obtain

$$\widetilde{W}(\bar{\mathbf{D}}) = \inf_{\boldsymbol{\Xi}} \left\{ \min_{\mathbf{D}\in K} \left[\int_\Omega \left(W^0(\mathbf{D}) + \boldsymbol{\Xi}\cdot\mathbf{D}\right)\,\mathrm{d}V\right] - \int_\Omega \left(W - W^0\right)^*(\mathbf{x},\boldsymbol{\Xi})\,\mathrm{d}V \right\}, \tag{A 5}$$

as first shown by Talbot & Willis (1985) in the context of linear elasticity. Now, taking the polarization stress field as given, it follows that the Euler-Lagrange equation for the "inner" minimum problem over the field $\mathbf{D}$ is given by

$$\eta^0\,\nabla^2\mathbf{v} - \boldsymbol{\nabla} p = -\boldsymbol{\nabla}\cdot\boldsymbol{\Xi}, \text{ and } \nabla\cdot\mathbf{v} = 0 \text{ in } \Omega, \text{ and } \mathbf{v} = \bar{\mathbf{L}}\mathbf{x} \text{ on } \partial\Omega. \tag{A 6}$$

The above differential equation corresponds to the Stokes equation for a homogeneous Newtonian fluid with viscosity η^0 subjected to the body force distribution $\boldsymbol{\nabla}\cdot\boldsymbol{\Xi}$ in the domain Ω, along with the affine condition $\mathbf{v} = \bar{\mathbf{L}}\mathbf{x}$ on the boundary $\partial\Omega$. After choosing η^0 to be equal to $\eta^{(1)}$, the above equations turns out to be the same as those considered by Gao *et al.* (2011) in the context of dilute suspensions. As discussed in section 3 of Gao *et al.* (2011), the solutions for the strain rate and vorticity fields in the domain Ω can be expressed in terms of the Green's function $\mathbf{G}(\mathbf{x},\mathbf{x}')$ as

$$D_{ij}(\mathbf{x}) = \bar{D}_{ij} + \int_{\Omega^{(2)}} \Gamma_{ijpq}(\mathbf{x},\mathbf{x}')\,\Xi_{pq}(\mathbf{x}')\,d\mathbf{x}', \quad \text{and} \tag{A 7}$$

$$W_{ij}(\mathbf{x}) = \bar{W}_{ij} + \int_{\Omega^{(2)}} \Lambda_{ijpq}(\mathbf{x},\mathbf{x}')\,\Xi_{pq}(\mathbf{x}')\,d\mathbf{x}', \tag{A 8}$$

respectively, where $\Gamma_{ijpq} = (\partial^2 G_{ip}/\partial x_j\,\partial x'_q)|_{(ij),(pq)}$ and $\Lambda_{ijpq} = (\partial^2 G_{ip}/\partial x_j\,\partial x'_q)|_{[ij],(pq)}$ with the parentheses and square brackets (enclosing indices) denoting symmetric and anti-symmetric parts, respectively. The above solution requires information on the polarization stress field in the particle phase (note that $\boldsymbol{\Xi}$ is zero in the matrix because of the choice $\eta^0 = \eta^{(1)}$.) For the case of dilute suspensions of ellipsoidal neo-Hookean

particles, it was shown by Gao *et al.* (2011), building on earlier work by Willis (1977) in linear elasticity, that the polarization field in the particles is uniform. On the other hand, for non-dilute suspensions, the polarization field is not expected to be uniform in the particles. However, again building on earlier work (Willis 1977; Ponte Castañeda & Willis 1995), it is reasonable to make use of piecewise constant polarization trial fields in the sense of a variational approximation. Thus, the use of the trial stress polarization $\boldsymbol{\Xi}(\mathbf{x}) = \chi^{(2)}(\mathbf{x})\,\boldsymbol{\Xi}^{(2)}$, where $\chi^{(2)}(\mathbf{x})$ is the characteristic function of the particle phase, and $\boldsymbol{\Xi}^{(2)}$ the corresponding (uniform) stress polarizations in the inclusion phase (recall that $\boldsymbol{\Xi}^{(1)} = \mathbf{0}$, due to the choice $\eta^0 = \eta^{(1)}$), leads to the result that

$$\widetilde{W}(\bar{\mathbf{D}}) \leq \inf_{\boldsymbol{\Xi}^{(2)}} \left\{ \min_{\mathbf{D}\in K} \left[\int_\Omega \left(W^0(\mathbf{D}) + \boldsymbol{\Xi}\cdot\mathbf{D} \right) \,\mathrm{d}V \right] - \int_\Omega \left(W - W^0 \right)^* (\mathbf{x}, \boldsymbol{\Xi})\,\mathrm{d}V \right\}. \quad \text{(A 9)}$$

Making use of this approximation of uniform polarizations in the particles, and under the *separation of length scales* and *no long-range order* hypotheses for the random distribution of the particle phase (Willis 1981; Ponte Castañeda & Willis 1995; Ponte Castañeda 2005), the tensors Γ_{ijpq} and Λ_{ijpq} in relations (A 7) and (A 8) may be replaced by the corresponding tensors constructed from the infinite-body Green's function. (In this connection, it should be noted that at sufficiently large particle concentrations, the later hypothesis may no longer be appropriate due to the possible development of quasi-periodic order in the microstructures, although such effects are beyond the scope of the model in its present form.) Then, for the case of ellipsoidal particles distributed with ellipsoidal symmetry (i.e., such that the two-point correlation functions for the distribution of the particle centers exhibit ellipsoidal angular dependence), it can be shown (Ponte Castañeda & Willis 1995; Ponte Castañeda 2005) that the averages over the particle phase of the strain rate and vorticity tensors in (A 7) and (A 8) are given by

$$\bar{\mathbf{D}}^{(2)} = \bar{\mathbf{D}} - (1-c)\,\mathbb{P}\,\boldsymbol{\Xi}^{(2)}, \qquad \bar{\mathbf{W}}^{(2)} = \bar{\mathbf{W}} - (1-c)\,\mathbb{R}\,\boldsymbol{\Xi}^{(2)}, \quad \text{(A 10)}$$

respectively, where $c = c^{(2)}$ is the volume fraction of the particle phase, and $\mathbb{P}$ and $\mathbb{R}$ are fourth-order microstructural tensors defined by

$$\mathbb{P} = \frac{1}{4\pi\,|\mathbf{Z}|} \int_{|\boldsymbol{\xi}|=1} \mathbb{H}(\boldsymbol{\xi})\,\left|\mathbf{Z}^T\boldsymbol{\xi}\right|^{-3} dS, \quad \text{and} \quad \mathbb{R} = \frac{1}{4\pi\,|\mathbf{Z}|} \int_{|\boldsymbol{\xi}|=1} \mathbb{T}(\boldsymbol{\xi})\,\left|\mathbf{Z}^T\boldsymbol{\xi}\right|^{-3} dS. \quad \text{(A 11)}$$

In these expressions, the fourth-order tensor $\mathbb{H}$ and $\mathbb{T}$ are in turn defined by

$$H_{ijkl} = \left(M_{ik}\xi_j\xi_l\right)\big|_{(ij)(kl)}, \qquad T_{ijkl} = \left(M_{ik}\xi_j\xi_l\right)\big|_{[ij](kl)}, \quad \text{(A 12)}$$

where $\mathbf{M} = \eta^{(1)}(\mathbf{I} - \boldsymbol{\xi}\otimes\boldsymbol{\xi})$.

Having solved for the strain-rate in the "inner" minimum problem, we next need to find the optimal (uniform) stress polarization $\boldsymbol{\Xi}^{(2)}$ in the inclusions. By evaluating the derivative of the integrals in (A 9) with respect to $\boldsymbol{\Xi}^{(2)}$, and solving for $\boldsymbol{\Xi}^{(2)}$, we obtain the result

$$\boldsymbol{\Xi}^{(2)} = \bar{\boldsymbol{\tau}}^{(2)} - 2\,\eta^{(1)}\,\bar{\mathbf{D}}^{(2)}, \quad \text{(A 13)}$$

where $\bar{\boldsymbol{\tau}}^{(2)}$ is the average of the extra stress in the particles at the current instant.

Substituting $\boldsymbol{\Xi}^{(2)}$, as determined by relation (A 13), in relations (A 10), we obtain the following expressions for the average strain rate and vorticity tensors in particles

$$\bar{\mathbf{D}}^{(2)} = \left[\mathbb{I} - 2(1-c)\,\eta^{(1)}\,\mathbb{P}\right]^{-1} \left\{\bar{\mathbf{D}} - (1-c)\mathbb{P}\,\bar{\boldsymbol{\tau}}^{(2)}\right\}, \quad \text{(A 14)}$$

and

$$\bar{\mathbf{W}}^{(2)} = \bar{\mathbf{W}} + (1-c)\,\mathbb{R}\,\left(2\,\eta^{(1)}\,\bar{\mathbf{D}}^{(2)} - \bar{\boldsymbol{\tau}}^{(2)}\right). \tag{A 15}$$

As mentioned earlier, in this work, we consider suspensions of KV particles with a linear viscous part ($\boldsymbol{\tau}_v^{(2)} = 2\eta^{(2)}\mathbf{D}$). It follows that the total average extra stress tensor in the KV particles reads as (see relation (2.1))

$$\bar{\boldsymbol{\tau}}^{(2)} = \bar{\boldsymbol{\tau}}_e^{(2)} + \bar{\boldsymbol{\tau}}_v^{(2)} = \bar{\boldsymbol{\tau}}_e^{(2)} + 2\,\eta^{(2)}\bar{\mathbf{D}}^{(2)}. \tag{A 16}$$

Then, making use of this decomposition in relations (A 14) and (A 15), we arrive at the results (3.18) and (3.19) for the averages of the strain rate and vorticity tensors, respectively, in the particles. With this result, it can be shown that the effective *pseudo*-dissipation potential (A 9) can be written in the form (3.17). Finally, it should be noted that under the assumption that $\eta^0 \geq \eta^{(1)}, \eta^{(2)}$, it follows from (A 9) that the right-hand side of (3.17) is a rigorous upper bound (see also Lahellec *et al.* 2011) for the effective *pseudo*-dissipation potential $\widetilde{W}(\bar{\mathbf{D}})$. On the other hand, if it is assumed instead that $\eta^0 \leq \eta^{(1)}, \eta^{(2)}$, the expression in the right-hand side of (3.17) can alternatively be shown to provide a lower bound for $\widetilde{W}(\bar{\mathbf{D}})$, even if the corresponding expressions for $\bar{\mathbf{D}}^{(2)}$ and $\bar{\boldsymbol{\tau}}_e^{(2)}$ do not change. However, in this work, we will not insist on the bounding properties of the estimate (3.17), and we make use of an equality in expression (3.17), in the sense of an approximation. It is also relevant to mention here that alternative variational approaches based directly on the minimum dissipation principle have been proposed to estimate the macroscopic instantaneous rheology of suspensions of rigid particles and high surface tension drops by Keller *et al.* (1967).

Appendix B. Governing equations for extensional flows

In this appendix, we present simplified evolution equations for the initially spherical particles subjected to the extensional flow defined by (5.1). Because of the flow symmetry, the initially spherical particles remain fixed in orientation, evolving into prolate spheroidal particles with aspect ratios $w = w_1 = w_2$. Also, the symmetry implies that $\bar{\tau}_{33}^{(2)} = \bar{\tau}_{22}^{(2)}$ and $\bar{D}_{22}^{(2)} = \bar{D}_{33}^{(2)} = -\bar{D}_{11}^{(2)}/2$, where the second equality follows from the incompressibility in the particles.

With the above-mentioned simplifications, and for the case of KV particles with Gent elastic behavior, the system of equations (3.18), (3.24), (3.27), and (A 16) can be shown to reduce to

$$\left.\begin{aligned}
&\frac{\mathrm{d}\bar{\tau}_{e11}^{(2)}}{\mathrm{d}\,t} = \frac{2}{\mu\,J_m}\bar{D}_{11}^{(2)}\,\left(\bar{\tau}_{e11}^{(2)}+\mu\right)\,\left(\bar{\tau}_{e11}^{(2)} - \bar{\tau}_{e22}^{(2)} + \mu\,Jm\right),\\
&\frac{\mathrm{d}\bar{\tau}_{e22}^{(2)}}{\mathrm{d}\,t} = -\frac{1}{\mu\,J_m}\bar{D}_{11}^{(2)}\,\left(\bar{\tau}_{e22}^{(2)}+\mu\right)\,\left[2\left(\bar{\tau}_{e22}^{(2)} - \bar{\tau}_{e11}^{(2)}\right) + \mu\,Jm\right],\\
&\bar{\tau}_{ij}^{(2)} = \bar{\tau}_{eij}^{(2)} + 2\,\eta^{(1)}\,\bar{D}_{ij}^{(2)}, \quad i,j=1,2,3, \qquad \frac{\mathrm{d}w}{\mathrm{d}t} = -\frac{3}{2}w\,\bar{D}_{11}^{(2)}\\
&\bar{D}_{11}^{(2)} = \frac{w^2\,(1-c)\left[(w^2+2)\omega_2 - 6\,\omega_1\right]\left(\bar{\tau}_{11}^{(2)} - \bar{\tau}_{22}^{(2)}\right) - 4\,\omega_1^5\,\eta^{(1)}\,\dot{\gamma}}{\left\{2\,\omega_1\left[9\,(1-c)\,w^2\,(\eta^{(2)}-\eta^{(1)}) - 2\,\omega_1^4\,\eta^{(1)}\right] - 3\,(1-c)\,w^2\,(w^2+2)\,\omega_2\,(\eta^{(2)}-\eta^{(1)})\right\}},
\end{aligned}\right\} \tag{B 1}$$

where $\omega_1 = \sqrt{1-w^2}$ and $\omega_2 = 2\,\ln(\omega_1+1) - 2\,\ln(w)$. Moreover, for the special case of neo-Hookean elastic response for the KV particles, the above system of ODEs for $\bar{\boldsymbol{\tau}}_e^{(2)}$

simplify further reducing to

$$\frac{\mathrm{d}\bar{\tau}^{(2)}_{e11}}{\mathrm{d}\,t} = 2\,\bar{D}^{(2)}_{11}\,\left(\bar{\tau}^{(2)}_{e11}+\mu\right), \qquad \frac{\mathrm{d}\bar{\tau}^{(2)}_{e22}}{\mathrm{d}\,t} = -\bar{D}^{(2)}_{11}\,\left(\bar{\tau}^{(2)}_{e22}+\mu\right), \tag{B 2}$$

while Eqs. (B 1)$_{3-5}$ remain the same.

Appendix C. Governing equations for shear flows

In this appendix, we provide simplified evolution equations for the initially spherical particles, when subjected to the shear flow conditions defined by (5.10). For simplicity, we provide equations only for the case of KV particles with neo-Hookean elastic response. Recall that the particles take on general ellipsoidal shapes characterized by the aspect ratios w_1 and w_2, but rotate only in the shear plane, the rotation being described by the angle θ. Then, the system of equations (3.24), (3.25), (3.27), and (A 16) can be shown to simplify to

$$\left.\begin{aligned}
&\dot{\bar{\tau}}^{(2)}_{e11} = 2(\bar{D}^{(2)}_{12}+\bar{W}^{(2)}_{12})\bar{\tau}^{(2)}_{e12} + 2\,(\bar{\tau}^{(2)}_{e11}+\mu)\bar{D}^{(2)}_{11},\\
&\dot{\bar{\tau}}^{(2)}_{e22} = 2(\bar{D}^{(2)}_{12}-\bar{W}^{(2)}_{12})\bar{\tau}^{(2)}_{e12} + 2\,(\bar{\tau}^{(2)}_{e22}+\mu)D^{(2)}_{22}, \quad \dot{\bar{\tau}}^{(2)}_{e33} = -2\,(\bar{\tau}^{(2)}_{e33}+\mu)(\bar{D}^{(2)}_{11}+\bar{D}^{(2)}_{22}),\\
&\dot{\bar{\tau}}^{(2)}_{e12} = (\bar{D}^{(2)}_{12}-\bar{W}^{(2)}_{12})\bar{\tau}^{(2)}_{e11} + (\bar{D}^{(2)}_{12}+\bar{W}^{(2)}_{12})\bar{\tau}^{(2)}_{e22} + \bar{\tau}^{(2)}_{e12}(\bar{D}^{(2)}_{11}+\bar{D}^{(2)}_{22}) + 2\,\mu\,\bar{D}^{(2)}_{12},\\
&\bar{\tau}^{(2)}_{ij} = \bar{\tau}^{(2)}_{eij} + 2\,\eta^{(2)}\,\bar{D}^{(2)}_{ij}, \qquad i,j=1,2,3\\
&\frac{\mathrm{d}w_1}{\mathrm{d}t} = -2\,w_1\,\bar{D}^{(2)}_{11}, \quad \frac{\mathrm{d}w_2}{\mathrm{d}t} = -w_2\,\bar{D}^{(2)}_{11}, \quad \frac{\mathrm{d}\theta}{\mathrm{d}t} = \left(\frac{1+w_1^2}{1-w_1^2}\right)\bar{D}^{(2)}_{12} - \bar{W}^{(2)}_{12}.
\end{aligned}\right\} \tag{C 1}$$

The above equations are complemented by relations (3.18) and (3.19) for the average strain rate $\bar{\mathbf{D}}^{(2)}$ and vorticity $\bar{\mathbf{W}}^{(2)}$ in the particles, respectively.

In the context of equations (C 1), it is noted that these equations are written relative to a fixed coordinate system which is instantaneously aligned with the principal axes of particles. As pointed out by Gao *et al.* (2011) (see Appendix A in that paper), because of the rotation of particles in shear flow, one must account for the rotation of this coordinate system in order to integrate the above system of equations. One simple way to account for this rotation is to express the stress tensor in the rotating principal axes of the particles (i.e., $\{\mathbf{n}_1,\mathbf{n}_2,\mathbf{n}_3\}$) as

$$\bar{\boldsymbol{\tau}}^{(2)}_{e} = \bar{\tau}^{(2)}_{e11}\,\mathbf{n}_1\,\mathbf{n}_1 + \bar{\tau}^{(2)}_{e22}\,\mathbf{n}_2\,\mathbf{n}_2 + \bar{\tau}^{(2)}_{e33}\,\mathbf{n}_3\,\mathbf{n}_3 + \bar{\tau}^{(2)}_{e12}\,(\mathbf{n}_1\,\mathbf{n}_2 + \mathbf{n}_2\,\mathbf{n}_1) \tag{C 2}$$

Taking the time derivative from both sides of the above relation, we can express the time derivative of the stress components in the fixed coordinates in terms of the time derivative of those in the rotating principal coordinates as (see relations (A 10) and (A 11) in Gao *et al.* (2011))

$$\begin{aligned}
&\dot{\bar{\tau}}^{(2)}_{e11} = \frac{\mathrm{d}\bar{\tau}^{(2)}_{e11}}{\mathrm{d}t} - 2\,\bar{\tau}^{(2)}_{e12}\,\frac{\mathrm{d}\theta}{\mathrm{d}t}, \quad \dot{\bar{\tau}}^{(2)}_{e22} = \frac{\mathrm{d}\bar{\tau}^{(2)}_{e22}}{\mathrm{d}t} + 2\,\bar{\tau}^{(2)}_{e12}\,\frac{\mathrm{d}\theta}{\mathrm{d}t},\\
&\dot{\bar{\tau}}^{(2)}_{e33} = \frac{\mathrm{d}\bar{\tau}^{(2)}_{e33}}{\mathrm{d}t}, \quad \dot{\bar{\tau}}^{(2)}_{e12} = \frac{\mathrm{d}\bar{\tau}^{(2)}_{e12}}{\mathrm{d}t} + (\bar{\tau}^{(2)}_{e11}-\bar{\tau}^{(2)}_{e22})\,\frac{\mathrm{d}\theta}{\mathrm{d}t}.
\end{aligned} \tag{C 3}$$

After substituting the above relations into the system of equations (C 1), we can directly apply an implicit (or explicit) time-discretization procedure to integrate the equations.

Appendix D. The tensors $\mathbb{P}$ and $\mathbb{R}$ for an ellipsoidal inclusion

In this appendix, explicit analytical expressions are given for the components of the tensors $\mathbb{P}$ and $\mathbb{R}$ for a general ellipsoidal particle suspended in an incompressible, isotropic, linear viscous matrix with the viscosity constant $\eta^{(1)}$. The final expressions for the components of the tensor $\mathbb{P}$ in the principal coordinate system of the particle read as (Eshelby 1957; Kailasam 1998)

$$\begin{aligned}
&\mathbb{P}_{1111} = h_1\,(6\,I_{11} - y_1),\ \ \mathbb{P}_{2222} = h_1\,(6\,I_{22}\,w_1^2 - y_2),\ \ \mathbb{P}_{3333} = h_1\,(6\,I_{33}\,w_2^2 - y_3),\\
&\mathbb{P}_{1122} = h_1\,(2\,w_1^2\,I_{12} - 3\,I_{11} - w_2^2\,I_{13}),\ \ \mathbb{P}_{1133} = h_1\,(2\,w_2^2\,I_{13} - 3\,I_{11} - w_1^2\,I_{12}),\\
&\mathbb{P}_{2233} = h_1\,(2\,w_2^2\,I_{23} - 3\,w_1^2\,I_{22} - I_{12}),\ \ \mathbb{P}_{1212} = h_2\,(1 + w_1^2)\,I_{12},\ \ \mathbb{P}_{1313} = h_2\,(1 + w_2^2)\,I_{13},
\end{aligned} \tag{D 1}$$

and $\mathbb{P}_{2323} = h_2\,(w_1^2 + w_2^2)\,I_{23}$ where $h_1 = (24\,\pi\,\eta^{(1)})^{-1}\,a^2$ and $h_2 = (16\,\pi\,\eta^{(1)})^{-1}\,a^2$. In the above expressions the following variables have also been introduced for brevity

$$y_1 = w_1^2\,I_{12} + w_2^2\,I_{13},\ \ y_2 = I_{12} + I_{23}\,w_2^2,\ \ y_3 = I_{13} + I_{23}\,w_1^2, \tag{D 2}$$

and the rest of the variables are defined as

$$\begin{aligned}
&I_1 = 4\,\pi\,w_1\,w_2\left[(1 - w_1^2)\,\sqrt{1 - w_2^2}\right]^{-1}(F - E),\quad I_2 = 4\,\pi - I_1 - I_3,\\
&I_3 = 4\,\pi\,w_1\,w_2\left[(w_1^2 - w_2^2)\,\sqrt{1 - w_2^2}\right]^{-1}\left[w_1\,w_2^{-1}\,\sqrt{1 - w_2^2} - E\right],\\
&I_{12} = \frac{1}{a^2(1 - w_1^2)}(I_2 - I_1),\ I_{13} = \frac{1}{a^2(1 - w_2^2)}(I_3 - I_1),\ I_{23} = \frac{1}{a^2(w_1^2 - w_2^2)}(I_3 - I_2),\\
&I_{11} = \frac{1}{3}(\frac{4\,\pi}{a^2} - I_{12} - I_{13}),\ I_{22} = \frac{1}{3}(\frac{4\,\pi}{a^2\,w_1^2} - I_{12} - I_{23}),\ I_{33} = \frac{1}{3}(\frac{4\,\pi}{a^2\,w_2^2} - I_{13} - I_{23}),
\end{aligned} \tag{D 3}$$

in which the functions F and E denote the incomplete elliptic integrals of the first and second kinds, respectively, and are defined as

$$F = \int_0^{\sin(\Theta)} \frac{1}{\sqrt{1 - t^2}\sqrt{1 - \kappa^2 t^2}}dt,\qquad E = \int_0^{\sin(\Theta)} \frac{\sqrt{1 - \kappa^2 t^2}}{\sqrt{1 - t^2}}dt, \tag{D 4}$$

where $\Theta = \sin^{-1}(\sqrt{1 - w_2^2})$, and $\kappa = \sqrt{1 - w_1^2}/\sqrt{1 - w_2^2}$. Moreover, the three independent components of the tensor $\mathbb{R}$ in the principal coordinate systems of the particle read as

$$\mathbb{R}_{ijij} = \frac{1}{16\,\pi\,\eta^{(1)}}\,(I_j - I_i),\quad \text{for } i, j = 1, 2, 3, \text{ and } j > i. \tag{D 5}$$

The remaining non-zero components of the tensor $\mathbb{R}_{ijkl}$ are obtained by recalling that this tensor is symmetric with respect to the first two indices ($\mathbb{R}_{jikl} = \mathbb{R}_{ijkl}$) and antisymmetric with respect to the last two indices ($\mathbb{R}_{ijlk} = -\mathbb{R}_{ijkl}$).

REFERENCES

Abreu, D., Levant, M., Steinberg, V. & Seifert, U. 2014 Fluid vesicles in flow. *Advances in Colloid and Interface Science* **208** (0), 129 – 141.

Almusallam, A.S., Larson, R.G. & Solomon, M.J. 2000 A constitutive model for the prediction of ellipsoidal droplet shapes and stresses in immiscible blends. *Journal of Rheology* **44** (5), 1055–1083.

Aravas, N. & Ponte Castañeda, P. 2004 Numerical methods for porous metals with deformation-induced anisotropy. *Comput. Meth. Appl. Mech. Engng.* **193**, 3767–3805.

Barthès-Biesel, D. 1980 Motion of a spherical microcapsule freely suspended in a linear shear flow. *J. Fluid Mech.* **100**, 831–853.

Barthès-Biesel, D. & Rallison, J. M. 1981 The time-dependent deformation of a capsule freely suspended in a linear shear flow. *J. Fluid Mech.* **113**, 251–267.

Batchelor, G. K. 1970 The stress system in a suspension of force-free particles. *J. Fluid Mech.* **41**, 545–570.

Batchelor, G. K. & Green, J.T. 1972 The determination of the bulk stress in a suspension of spherical particles to order c^2. *J. Fluid Mech.* **56**, 401–427.

Bernstein, B. 1960 Hypo-elasticity and elasticity. *Archive for Rational Mechanics and Analysis* **6** (1), 89–104.

Bilby, B. A., Eshelby, J.D. & Kundu, A. K. 1975 The change of shape of a viscous ellipsoidal region embedded in a slowly deforming matrix having a different viscosity. *Tectonophysics* **28**, 265–274.

Bilby, B. A. & Kolbuszewski, M. L. 1977 The finite deformation of an inhomogeneity in two-dimensional slow viscous incompressible flow. *Proc. R. Soc. Lond. A.* **355**, 335–353.

Brady, JF & Bossis, G 1985 The rheology of concentrated suspensions of spheres in simple shear flow by numerical simulation. *J. Fluid Mech.* **155** (JUN), 105–129.

Brady, J.F., Khair, A. S. & Swaroop, M. 2006 On the bulk viscosity of suspensions. *Journal of Fluid Mechanics* **554**, 109–123.

Brooks, D.E., Goodwin, J.W. & Seaman, G.V. 1970 Interactions among erythrocytes under shear. *J. Appl. Physiol.* **28** (2), 172–177.

Cerf, R. 1952 On the frequency dependence of the viscosity of high polymer solutions. *J. Chem. Phys.* **20**, 395–402.

Chen, H-S. & Acrivos, A. 1978 The effective elastic moduli of composite materials containing spherical inclusions at non-dilute concentrations. *International Journal of Solids and Structures* **14** (5), 349 – 364.

Clausen, J.R. & Aidun, C.K. 2010 Capsule dynamics and rheology in shear flow: Particle pressure and normal stress. *Phys. Fluids* **22**, 123302.

Clausen, J.R., Reasor, D.A. & Aidun, C.K. 2011 The rheology and microstructure of concentrated non-colloidal suspensions of deformable capsules. *J. Fluid Mech.* **685**, 202–234.

Danker, G. & Misbah, C. 2007 Rheology of a dilute suspension of vesicles. *Phys. Rev. Lett.* **98**, 088104.

Einstein, A. 1906 A new determination of molecular dimensions. *Ann. Physik* **19**, 289–306.

Ekeland, I. & Témam, R. 1999 *Convex Analysis and Variational Problems*. Philadelphia, PA: SIAM.

Eshelby, J.D. 1957 The determination of the elastic field of an ellipsoidal inclusion and related problems. *Proc. R. Soc. Lond. A* **241**, 376–396.

Frankel, N.A. & Acrivos, A. 1967 On the viscosity of a concentrated suspension of solid spheres. *Chem. Eng. Sci.* **22**, 847–853.

Fröhlich, H. & Sack, R. 1946 Theory of the rheological properties of dispersions. *Proc. R. Soc. Lond. A* **185**, 415–430.

Gadala-Maria, F. & Acrivos, A. 1980 Shear-induced structure in a concentrated suspension of solid spheres. *Journal of Rheology* **24** (6), 799–814.

Gao, T., Hu, H.H. & Ponte Castañeda, P. 2011 Rheology of a suspension of elastic particles in a viscous shear flow. *J. Fluid Mech.* **687**, 209–237.

Gao, T., Hu, H.H. & Ponte Castañeda, P. 2012 Shape dynamics and rheology of soft elastic particles in a shear flow. *Phys. Rev. Lett.* **108**, 058302.

Gao, T., Hu, H.H. & Ponte Castañeda, P. 2013 Dynamics and rheology of elastic particles in an extensional flow. *J. Fluid Mech.* **715**, 573–596.

Gent, A.N. 1996 A new constitutive relation for rubber. *Rubber Chem. Tech.* **69**, 59–61.

Ghigliotti, G., Biben, T. & Misbah, C. 2010 Rheology of a dilute two-dimensional suspension of vesicles. *J. Fluid Mech.* **653**, 489–518.

Goddard, J.D. & Miller, C. 1967 Nonlinear effects in the rheology of dilute suspensions. *J. Fluid Mech.* **28**, 657–673.

Goddard, J. D 1977 An elastohydrodynamic theory for the rheology of concentrated suspensions of deformable particles. *J. Non-Newton. Fluid* **2** (2), 169–189.

Hashin, Z. & Shtrikman, S. 1963 A variational approach to the theory of the elastic behavior of multiphase materials. *J. Mech. Phys. Solids* **11**, 127–140.

Jeffery, G. B. 1922 The motion of ellipsoidal particles immersed in a viscous fluid. *Proc. R. Soc. Lond. A* **102**, 161–179.

Jeffrey, D.J. & Acrivos, A. 1976 The rheological properties of suspensions of rigid particles. *AIChE Journal* **22**, 417–432.

Joseph, D.D. 1990 *Fluid Dynamics of Viscoelastic Liquids*. New York, NY: Springer-Verlag.

Kailasam, M 1998 A general constitutive theory for particulate composites and porous materials with evolving microstructures. PhD thesis, University of Pennsylvania.

Kailasam, M. & Ponte Castañeda, P. 1998 A general constitutive theory for linear and nonlinear particulate media with microstructure evolution. *J. Mech. Phys. Solids* **46** (3), 427–465.

Kailasam, M., Ponte Castañeda, P. & Willis, J.R. 1997 The effect of particle size, shape, distribution and their evolution on the constitutive response of nonlinearly viscous composites. I. Theory. *Phil. Trans. R. Soc. Lond. A* **355**, 1835–1852.

Keller, J. B., Rubenfeld, L. A. & Molyneux, J. E. 1967 Extremum principles for slow viscous flows with applications to suspensions. *Journal of Fluid Mechanics* **30** (01), 97–125.

Keller, S.R. & Skalak, R. 1982 Motion of a tank-treading ellipsoidal particle in a shear flow. *J. Fluid Mech.* **120**, 27–47.

Krieger, I.M. & Dougherty, T.J. 1959 A mechanism for non-newtonian flow in suspensions of rigid spheres. *J. Rheology* **3**, 137.

Lac, E., Barthès-Biesel, D., Pelekasis, N.A. & Tsamopoulos, J. 2004 Spherical capsules in three-dimensional unbounded stokes flows: effect of the membrane constitutive law and onset of buckling. *J. Fluid Mech.* **516**, 303–334.

Lahellec, N., Ponte Castañeda, P. & Suquet, P. 2011 Variational estimates for the effective response and field statistics in thermoelastic composites with intra-phase property fluctuations. *Proc. R. Soc. Lond. A* **467** (2132), 2224–2246.

Lowenberg, M. & Hinch, E.J. 1996 Numerical simulation of concentrated emulsion in shear flow. *J. Fluid Mech.* **321**, 395–419.

Milton, G.W. 2002 *The Theory of Composites*. Cambridge, UK: Cambridge University Press.

Ogden, R.W., Saccomandi, G. & Sgura, I. 2004 Fitting hyperelastic models to experimental data. *Comput. Mech.* **34**, 484–502.

Oldroyd, J. G. 1953 The elastic and viscous properties of emulsions and suspensions. *Proc. R. Soc. Lond. A* **218**, 122–132.

Pal, R. 2003 Rheology of concentrated suspensions of deformable elastic particles such as human erythrocytes. *J. Biomech.* **36**, 981–989.

Pal, R. 2010 *Rheology of Particulate Dispersions and Composites*. CRC Press.

Palierne, J.F. 1990 Linear rheology of viscoelastic emulsions with interfacial-tension. *Rheologica Acta* **29** (3), 204–214.

Phung, T.N., Brady, J.F. & Bossis, G. 1996 Stokesian dynamics simulations of brownian suspensions. *J. Fluid Mech.* **313**, 181–207.

Ponte Castañeda, P. 2005 *Heterogeneous Materials. Lecture Notes*. Department of Mechanics, Ecole Polytechnique.

Ponte Castañeda, P. & Suquet, P. 1998 Nonlinear composites. *Adv. Appl. Mech.* **34**, 171–302.

Ponte Castañeda, P. & Willis, J. R. 1995 The effect of spatial distribution on the effective behavior of composite materials and cracked media. *J. Mech. Phys. Solids* **43** (12), 1919–1951.

Ramanujan, S. & Pozrikidis, C. 1998 Deformation of liquid capsules enclosed by elastic membranes in simple shear flow: large deformations and the effect of fluid viscosities. *J. Fluid Mech.* **361**, 117–143.

Roscoe, R. 1967 On the rheology of a suspension of viscoelastic spheres in a viscous liquid. *J. Fluid Mech.* **28**, 273–293.

Saito, N. 1950 Concentration dependence of the viscosity of high polymer solutions.I. *Journal of The Physical Society of Japan* **5** (1), 4–8.

Skalak, R., Ozkaya, N. & Skalak, T.C. 1989 Biofluid mechanics. *Annu. Rev. Fluid. Mech.* **21**, 167–200.

Snabre, P. & Mills, P. 1999 Rheology of concentrated suspensions of viscoelastic particles. *Colloids Surf., A* **152**, 79–88.

Stickel, J.J. & Powell, R.L. 2005 Fluid mechanics and rheology of dense suspensions. *Annu. Rev. Fluid Mech.* **37**, 129–149.

Talbot, D.R.S. & Willis, J.R. 1985 Variational Principles for Inhomogeneous Non-linear Media. *IMA J Appl Math* **35**, 39–54.

Taylor, G. I. 1932 The viscosity of a fluid containing small drops of another fluid. *Proc. R. Soc. Lond. A* **138**, 41–48.

Tucker, C. L. & Moldenaers, P. 2002 Microstructural evolution in polymer blends. *Annual Review of Fluid Mechanics* **34** (1), 177–210.

Villone, M.M., Hulsen, M.A., Anderson, P.D. & Maffettone, P.L. 2014 Simulations of deformable systems in fluids under shear flow using an arbitrary lagrangian eulerian technique. *Computers & Fluids* **90**, 88 – 100.

Vlahovska, P.M., Blawzdziewicz, J. & Loewenberg, M. 2009 Small-deformation theory for a surfactant-covered drop in linear flows. *Journal of Fluid Mechanics* **624**, 293–337.

Wetzel, E. D. & Tucker, C. L. 2001 Droplet deformation in dispersions with unequal viscosities and zero interfacial tension. *J. Fluid Mech.* **426**, 199–228.

Willis, J.R. 1977 Bounds and self-consistent estimates for the overall moduli of anisotropic composites. *J. Mech. Phys. Solids* **25**, 185–202.

Willis, J.R. 1981 Variational and related methods for the overall properties of composites. *Adv. Appl. Mech.* **21**, 1–78.

Zhao, H. & Shaqfeh, E.S.G. 2013 The dynamics of a non-dilute vesicle suspension in a simple shear flow. *Journal of Fluid Mechanics* **725**, 709–731.